Mechanisms for the Influence from Ice Nucleus Aerosols on Clouds and their Indirect Effects: Cloud Modelling

DEEPAK WAMAN
DEPARTMENT OF PHYSICAL GEOGRAPHY AND ECOSYSTEM SCIENCE | LUND UNIVERSITY

A significant amount of global precipitation is linked to the formation of ice particles in clouds. In addition, ice microphysical processes affect the Earth's radiation budget. The presence of ice in clouds is a culmination of many complex processes that are still poorly understood. The role of clouds containing ice on global radiation and hydrological budgets is highly uncertain.

In this thesis, the author examines the importance of various ice microphysical processes in mixed-phase clouds using numerical model simulations. It is found that the ice nucleation activity of various biological particles, as well as the time-dependent freezing of ice nucleating particles (INPs), have a minimal effect on the properties of mixed-phase clouds. For the first time, the relative importance of four secondary ice production mechanisms is investigated in various cloud types. Moreover, the thesis investigates how an increase in aerosols through anthropogenic activities leads to changes in cloud radiative properties. Also, this study newly discovered two new indirect effects arising from SIP and from time dependence of INP freezing.

Dr. Sachin G. Patade
(Researcher, INES, Lund University)

Printed by Media-Tryck, Lund 2023 NORDIC SWAN ECOLABEL 3041 0903

Lund University

Department of Physical Geography
and Ecosystem Science
Faculty of Science

ISBN 978-91-89187-25-2

MECHANISMS FOR THE INFLUENCE FROM ICE NUCLEUS AEROSOLS ON CLOUDS AND THEIR INDIRECT EFFECTS: CLOUD MODELLING

Mechanisms for the Influence from Ice Nucleus Aerosols on Clouds and their Indirect Effects: Cloud Modelling

Deepak Waman

LUND UNIVERSITY

DOCTORAL DISSERTATION

Doctoral dissertation for the degree of Doctor of Philosophy (PhD) at the Faculty of Science at Lund University to be publicly defended on 06th of October 2023 at 13.00 in Världen Hall, Department of Physical Geography and Ecosystem Science, Sölvegatan 12, Lund, Sweden

Faculty opponent
Professor Andrea Flossmann
University of Clermont Auvergne, France

Organization Lund University Faculty of Science Department of Physical Geography and Ecosystem Science Author: Deepak Meera Balasaheb Waman	**Document name** DOCTORAL DISSERTATION **Date of issue** 06 October 2023 Sponsoring organization
Title and subtitle Mechanisms for the Influence from Ice Nucleus Aerosols on Clouds and their Indirect Effects: Cloud Modelling	

Abstract

The role of multiple groups of primary biological aerosol particles (PBAPs) as ice nucleating particles (INPs), and of ice formation processes such as time-dependent freezing of various INPs, and various secondary ice production (SIP) mechanisms in overall ice concentration has been evaluated in a range of cloud systems by simulating them numerically with the state-of-the-art 'Aerosol-Cloud' (AC) model in a 3D mesoscale domain. Also, the mechanisms of aerosol indirect effects (AIEs) arising from anthropogenic INPs, and the responses to these AIEs from time-dependent INP freezing and SIP processes are investigated in the simulated clouds. The cloud systems simulated with AC are: events of summertime deep convection observed over Oklahoma, USA during the Midlatitude Continental Convective Cloud Experiment (MC3E) in 2011 on 1) 11 May, and 2) 20 May, and wintertime 3) orographic clouds observed during the Atmospheric Radiation Measurement Cloud Aerosol Precipitation Experiment (ACAPEX) on 07 February 2015 over North California, and 4) supercooled layer clouds observed over Larkhill, UK, during the Aerosol Properties, Processes And Influences on the Earth's climate (APPRAISE) campaign on 18 February 2009.

AC uses the dynamical core of the Weather Research and Forecasting (WRF) model, modified Geophysical Fluid Dynamic Laboratory (GFDL) radiation scheme, and hybrid bin-bulk microphysics scheme. AC is validated adequately with the coincident aircraft, ground-based, and satellite observations for all four cases. AC forms secondary ice through the Hallett-Mossop (HM) process of rime-splintering, and fragmentation during ice-ice collisions, raindrop freezing, and sublimation of dendritic snow and graupel. A measure of SIP is defined using the term 'ice enhancement' (IE) ratio which is the ratio between the number concentration of total ice particles and active INPs at cloud tops.

For both cases in MC3E, overall, PBAPs have little effect (+1-6%) on the cloud-liquid (droplet mean sizes, number concentrations, and their water contents) properties, overall ice concentration, and on precipitation. AC predicts the activity of various INPs with an empirical parameterization (EP). The EP is modified to represent the time-dependent approach of INP freezing in light of our published laboratory observations. It is predicted that the time dependence of INP freezing is not the main cause for continuous ice nucleation and precipitation in all simulated cases. Rather, the main mechanism of precipitation formation is the combination of various SIP mechanisms (in convection) and recirculation-reactivation of dust particles (in APPRAISE layer cloud episode). Also, for all cases, the inclusion of time dependence of INP freezing causes little increase (about 10-20%) in the total ice concentration and ice from all SIP.

Regarding SIP, in young developing convective clouds of MC3E (11 May), with tops > -15^{o}C, the initial explosive growth is from the fast HM process, creating IE ratios as high as 10^3. By contrast, in mature convective clouds (tops < -20^{o}C), fragmentation in ice-ice collisions prevails, creating IE ratios of up to about 10^2-10^3. Regarding AIEs from INPs, increasing anthropogenic pollution is predicted to exert a net cooling in APPRAISE, and a strong net warming in MC3E (11 May). Furthermore, these net AIEs are mainly from glaciated clouds. Overall, the contribution to the AIEs from ice formation processes, such as time-dependent INP freezing and SIP, shows a high sensitivity with respect to anthropogenic INPs (about 20-60% increase in net AIEs).

Also, two new indirect effects associated with ice initiation mechanisms are proposed here. These are, 1) the 'SIP' indirect effect, and 2) the 'time-dependent INP' indirect effect. It is predicted that in APPRAISE and MC3E, both SIP and time-dependent INP indirect effects form less than 30%, and more than 50% of the net AIE, respectively.

Key words: Clouds, Ice Nucleating Particles, Primary ice, Secondary ice, Aerosol indirect effects, Cloud radiative effects, Aerosol-Cloud interactions, Cloud Resolving Model		
Classification system and/or index terms (if any)		
Supplementary bibliographical information	**Language** English	
ISSN and key title	**ISBN** 978-91-89187-25-2 (print) 978-91-89187-26-9 (electronic)	
Recipient's notes	**Number of pages**	Price
	Security classification	

Signature Date 06 October 2023

Mechanisms for the Influence from Ice Nucleus Aerosols on Clouds and their Indirect Effects: Cloud Modelling

Deepak Waman

LUND UNIVERSITY

Faculty of Science

Department of Physical Geography and Ecosystem Science

ISBN (print) 978-91-89187-25-2

ISBN (electronic) 978-91-89187-26-9

Printed in Sweden by Media-Tryck, Lund University, Lund 2023

NORDIC SWAN ECOLABEL
Printed matter 3041 0903

Media-Tryck is a Nordic Swan Ecolabel certified provider of printed material. Read more about our environmental work at www.mediatryck.lu.se

MADE IN SWEDEN

To my beloved family…

निश्चयाचा महामेरू। बहुत जनासी आधारू।
अखंडस्थितीचा निर्धारू। श्रीमंत योगी॥

अनन्याश्चिन्तयन्तो मां ये जनाः पर्युपासते।
तेषां नित्याभियुक्तानां योगक्षेमं वहाम्यहम्॥ ९-२२॥

Ananyash Chintayanto Mam Ye Janah Paryupasate |
Tesham Nityabhiyuktanam Yoga-Kshemam Vahamyaham ||9–22||

"जे अनन्य प्रेमी दास मज परमेश्वराला निरंतर चिंतन करीत निष्काम भावाने भजतात, त्या नित्य माझे चिंतन करणाऱ्यांचा योगक्षेम मी स्वतः त्यांना प्राप्त करून देतो. ॥ ९-२२ ॥"

"There are those who always think of Me and engage in exclusive devotion to Me. To them, whose minds are always absorbed in Me, I provide what they lack and preserve what they already possess. ||9-22||"

"वेडात जा पुढे तू, शोधीत मुक्त तारे|
पायाखालील काटे, होतील व्यर्थ सारे||
फिकीर सोड आता, ऋतू कोणता लाभला|
सारेच देणे त्याचे, तू डाव फक्त मांडला||
आता नको मशाल ती, चटक्यांची उगी सोबत|
मिणमिणती ती पणती, दुरून झोडी नौबत||
स्पंदने अगणिक मनाचे, अव्यक्त आणि स्तब्ध|
आरक्त नयन आता, होतील तेच शब्द||
खलात गुरफटले आयुष्य, उरले ना जरी काही|
धमन्यात रुधिर वाहते, दे झुगारून बेबंदशाही||
असुदे आता कितीही, भयाण वादळवारा|
मस्तीत पुढे तू चाल, हो निढळ ध्रुवतारा||"
...दीपक

Contents

List of Papers

Paper *1*

Patade, S., **Waman, D.**, Deshmukh, A., Gupta, A.K., Jadav, A., Phillips, V.T., Bansemer, A., Carlin, J. and Ryzhkov, A., 2022. The influence of multiple groups of biological ice nucleating particles on microphysical properties of mixed-phase clouds observed during MC3E. *Atmospheric Chemistry and Physics*, *22*(18), pp.12055-12075. https://doi.org/10.5194/acp-22-12055-2022.

Paper 2

Waman, D., Deshmukh, A., Jadav, A., Patade, S., Gautam, M., Phillips, V., Bansemer, A. and Jakobsson, J., 2023. Effects from time dependence of ice nucleus activity for contrasting cloud types. *Journal of the Atmospheric Sciences*. https://doi.org/10.1175/JAS-D-22-0187.1.

Paper 3

Waman, D., Patade, S., Jadav, A., Deshmukh, A., Gupta, A.K., Phillips, V.T., Bansemer, A. and DeMott, P.J., 2022. Dependencies of Four Mechanisms of Secondary Ice Production on Cloud-Top Temperature in a Continental Convective Storm. *Journal of the Atmospheric Sciences*, *79*(12), pp.3375-3404. https://doi.org/10.1175/JAS-D-21-0278.1.

Paper 4

Waman, D., Deshmukh, A., Jadav, A., Patade, S., Gautam, M., Phillips, V., 2023: Mechanisms for Indirect Effects from Solid Aerosol Particles on Continental Clouds and Radiation. *Manuscript submitted to the Journal of the Atmospheric Sciences*.

Author contributions

Paper 1

SP and VTJP designed and conceptualized this study. SP and **DW** set-up the simulation and performed the model validation. SP and **DW** processed the observational data from the aircraft and ground-based instruments. SP wrote the paper with contributions from the other authors. VTJP acquired the funding.

Paper 2

DW and VTJP conceptualized the study. **DW** with the help from VTJP and SP modified the model parameterization for heterogeneous ice initiation to represent time dependent approach of ice nucleus freezing. **DW** analyzed the aircraft data, set-up the model together with the other authors and carried out model simulations. **DW** wrote the paper with contributions from the other authors. VTJP acquired the funding.

Paper 3

DW conceptualized this study with guidance from VTJP. **DW** set-up and developed the model and carried out the model validation with the help from AJ and SP. **DW** analyzed the observational data from aircraft and ground-based instruments. **DW** wrote the paper with contributions from the other authors. VTJP acquired the funding.

Paper 4

DW designed and conceptualized this study with guidance from VTJP. **DW** developed the model and carried out simulations. **DW** drafted the manuscript and revised the manuscript with the help from the other authors. VTJP acquired the funding.

Popular Science Summary

This study on the ice phase of the clouds discovered that in continental conditions, the ice nucleating ability of groups of PBAPs is relatively weak compared to mineral dust and soot aerosols. The time-dependent freezing of available INPs is found to have a minimal impact on the overall ice concentration in the simulated cloud systems. Instead, a combination of various ice multiplication mechanisms plays a key role in the quasi-steady ice formation and precipitation over several hours in cloud systems that are convective. This study also revealed that in long-lived layer clouds, recirculation and subsequent reactivation of dust particles, rather than time-dependent INP freezing, is the main source for continuous ice nucleation and precipitation. Also, it is the coordinated combination of various SIP that accurately explains the observed discrepancy between the number concentrations of active INPs and total ice particles. Moreover, this study also explains the role of various SIP mechanisms in the observed dependency of ice enhancement ratio on cloud top temperature in the different stages of the convective clouds. Additionally, this study demonstrated that anthropogenically boosted solid APs can have a substantial impact on cloud micro- and macrophysical as well as radiative properties. The presence of extra INPs in the present-day conditions also causes perturbations in the processes of ice formation (SIP and time-dependent INP freezing), affecting the net solid aerosol indirect effects, mainly from glaciated clouds. This study also found that the indirect effects of solid aerosols are strongly dependent on the cloud system. For example, the inclusion of extra INPs predicts a net cooling of the climate system from supercooled stratiform clouds and strong warming from deep convective clouds.

Populärvetenskaplig sammanfattning

Denna studie om molnmikrofysik upptäckte att i kontinentala förhållanden är isnukleationsförmågan hos grupper av PBAPs relativt svag jämfört med mineraliskt damm och sotpartiklar. Den tidsberoende frysningen av tillgängliga INPs visade sig ha en minimal påverkan på den övergripande iskoncentrationen i de simulerade molnsystemen. Istället spelar en kombination av olika mekanismer för ismångfald en nyckelroll i den kvasi-stabila isbildningen och nederbörden under flera timmar i konvektiva molnsystem. Denna studie avslöjade också att i långlivade skiktmoln utan konvektion är recirkulation och efterföljande återaktivering av dammpartiklar, snarare än tidsberoende INP frysning, den huvudsakliga källan till kontinuerlig isnukleation och nederbörd. Dessutom är det den samordnade kombinationen av olika SIP mekanismer som noggrant förklarar den observerade avvikelsen mellan antalet aktiva INPs och totala ispartiklar. Vidare förklarar denna studie också rollen som olika SIP mekanismer spelar för den observerade beroendet av IE-förhållandet på molnens topptemperatur i olika stadier av konvektiva moln. Dessutom visade denna studie att antropogent förstärkta fasta AP:er kan ha en betydande påverkan på molnens mikro- och makrofysiska samt strålningsmässiga egenskaper. Förekomsten av extra INP:er under dagens förhållanden orsakar också störningar i processerna för isbildning (SIP och tidsberoende INP frysning), vilket påverkar de nettoindirekta effekterna från fasta aerosoler, främst från glaciärmoln. Denna studie fann också att de indirekta effekterna av fasta aerosoler är starkt beroende av molnsystemet. Till exempel förutsäger inkludering av extra INPs en nettoavkylning av klimatsystemet från underkylt skiktmoln och en kraftig uppvärmning från djupa konvektiva moln.

Acknowledgement

My profound gratitude extends to all of the individuals from different organizations, who have contributed to the completion of this doctoral thesis work. Their unwavering guidance, support, encouragement, and advice have been phenomenal in shaping this work. First and foremost, I would like to express my sincere gratitude to my supervisor, Dr. Vaughan T. J. Phillips for his priceless assistance, support and guidance throughout my Ph.D. journey. I would also like to extend my gratitude to my department representatives, Prof. Jonas Ardö, Prof. Paul Miller, and Prof. Thomas Kristensen for assessing and ensuring the quality of my work.

I would also like to acknowledge the following people for their contribution to the published and submitted research articles: Aaron Bansemer (for providing the aircraft data and for his valuable insights on the scientific challenges during the model validation), Dr. Paul DeMott (for providing the observations of INPs to validate the model), Dr. Jonas Jakobsson (for his suggestions during the implementing the formulation for the time dependence of INP freezing in the model), Dr. Jonathan Crosier, Prof. Paul Connolly, Prof. Ken Carslaw, Dr. Larry Horowitz, and Dr. Mian Chin (for their helpful suggestions to use the appropriate aerosol data to simulate a cloud case). Also, special thanks to all my co-authors for sharing their valuable knowledge and expertise. I would further like to express my sincere gratitude to Dr. Sachin Patade, Neelam Malap, Dr. Gayatri Kulkarni, Dr. Chandra Sekhar Pant, Dr. Freddy Paul, and Martanda Gautam for nurturing a strong friendship bond, and for their priceless guidance. Your support has been truly invaluable!

Also, I am heavily indebted to Dr. Sachin and Sonali Patade for their relentless support, guidance, and unwavering belief in my abilities throughout this research journey. Your constant encouragement and presence have been an invaluable source of strength and motivation that excelled me forward, even during the most challenging times. I have no adequate words to express my gratitude for your faith in me. And how I can erase the wonderful memories I have crafted during my stay with you, Dr. Sanjay and Varsha Borhade, special thanks to both of you and also to Manohar and Sarika Salunkhe, and Chakane family, I will miss celebrating festivals with you. To Advika, Sharvil, Manas, Manaswi, Swaroop, and Shweta, your presence has been a haven of joy for me. Spending time and playing with you has truly embraced my inner child and has created unforgettable memories.

I would like to take this opportunity to express my sincere gratitude to many people from my hometown and from my bachelor's college without whom I could not be able to achieve this. My sincere gratitude to Dr. Sanjay Malpani, an embodiment of inspiration and support for many students, and also to Dr. S. Dalvi, Dr. S. Arote, Dr. P. Bardapurkar, Dr. B. Palve, Dr. S. Navale, Dr. D. Gapale, Dr. P. Bawiskar, Dr. R.

Waykar, and all teaching, non-teaching staff of the Department of Physics, Sangamner College for their constant encouragement and support during my bachelor degree and during tough times afterward.

My sincere gratitude to Prof. Anandkumar Karipot, Prof. P. Pradeep Kumar, Dr. P. Sen, Dr. Sinha Ray, and the entire compassionate community from the Department of Atmospheric and Space Sciences, Pune University, and to Dr. B. S. Murthy, Dr. R. Latha from the Indian Institute of Tropical Meteorology (IITM), Pune. Your unwavering support has been instrumental and nurturing my growth in this field. I would further like to extend my gratitude to Dr. Thara Prabhakaran of the IITM, Pune, whose work on clouds always motivated me to pursue my career in this field.

My gratitude is further addressed to all my colleagues and friends at the Department of Physical Geography and Ecosystem Science. Special thanks to Arti Jadav, Dr. Joel White, Johan Eckdahl, Dr. Ushnanshu Dutta, Dr. Mahendra Pal, and Dr. Abhishek Lodh for sharing good times. I really enjoyed your company. My special thanks to all my friends from my hometown, Sangamner College, and Pune University, your constant support in tough times was invaluable!

Finally, this work would not have been completed without the support and love of my family. I sincerely express my heartfelt gratitude to my dear parents, you are the center of my world! I will forever cherish the way you taught me how to face challenges in life. Your hard work and unwavering dedication to run our family has always encouraged me to pursue my education against all odds. To my beloved brother, Pradip, you are an embodiment of inspiration! Your support, guidance, and faith in me have been an invaluable asset throughout this journey. Your fearless approach to confront any situation has always been a source of courage for me. A common thread that strongly binds my family together is my sister-in-law, Manjushree, I express my heartfelt appreciation to you for your contributions. And, dear Pratima, your presence has illuminated a previously undiscovered corner of my life, filling it with a profound sense of fulfillment and wholeness. A lot of love!

List of Figures

List of Tables

List of Abbreviations

2DC	2-Dimensional Cloud probe
2DS	2-Dimensional Spectrometer
AC	Aerosol-Cloud model
ACAPEX	Atmospheric Radiation Measurement Cloud Aerosol Precipitation Experiment
AIEs	Aerosol Indirect Effects
AMF2	ARM Facility 2
APs	Aerosol Particles
APPRAISE	Aerosol Properties, Processes And Influences on the Earth's climate
ARM	Atmospheric Radiation Measurement
CAPE	Convective Available Potential Energy
CCN	Cloud Condensation Nuclei
CDP	Cloud Droplet Probe
CF	Central Facility
CFARR	Chilbolton Facility for Atmospheric and Radio Research
CIP	Cloud Imaging Probe
CRE	Cloud Radiative Effect
CRM	Cloud Resolving Model
DMT	Droplet Measurement Technique
DoE	Department of Energy
EP	Empirical Parameterization
GFDL	Geophysical Fluid Dynamic Laboratory
GPM	Global Precipitation Measurement
HM	Hallett-Mossop
HVPS	High Volume Precipitation Spectrometer
HYSPLIT	Hybrid Single-Particle Lagrangian Integrated Trajectory
IE	Ice Enhancement
INPs	Ice Nucleating Particles
IWC	Ice Water Content
LCL	Lifting Condensation Level
LSF	Large Scale Forcing
LW	Longwave radiation
LWC	Liquid Water Content
MC3E	Midlatitude Continental Convective Cloud Experiment
MCS	Mesoscale Convective System
MSL	Mean Sea Level
NASA	National Aeronautics and Space Administration
NOAA	National Oceanic and Atmospheric Administration
NSF	National Science Foundation
PBAPs	Primary Biological Aerosol Particles

PBL	Planetary Boundary Layer
SGP	Southern Great Plains
SIP	Secondary Ice Production
SW	Shortwave radiation
UND	University of North Dakota
UTC	Coordinated Universal Time
WRF	Weather Research and Forecasting

List of Symbols

Symbol	Description	Unit
X	Aerosol species (X= dust, soot, soluble organic, fungi, pollen, bacteria, algae, detritus)	-
A_X	Proportionality constant for a power law dependence of temperature shift of time	$\mathrm{Ks}^{-\beta}$
T	Temperature of ambient air	ºC
S_i	Saturation ratio of vapor with respect to (w. r. t.) ice	-
S_i^w	Value of S_i at water saturation	-
S_w	Saturation ratio of vapor w. r. t. (plane) water	-
s_w	Supersaturation of vapor w. r. t. water	%
s_i	Supersaturation of vapor w. r. t. ice ($s_i = 100 \times [S_i - 1]$)	%
D_X	Diameter of a given aerosol species	μm
H_X	Fraction reducing INP activity at warm T and low S_i for various groups of aerosols in X	-
n_i	Number mixing ratio (m. r.) of ice crystals generated from EP	kg^{-1}
$n_{IN,1,*}$	Background-tropospheric reference activity spectrum number m. r. for water saturation	kg^{-1}
$n_{IN,rain}$	Number m. r. of rain's activated INP	kg^{-1}
$n_{IN,X}$	Number m. r. of X INP species from the EP	kg^{-1}
n_X	Number m. r. of APs in group of X (not depleted by ice nucleation while inside the cloud)	kg^{-1}
$n_{X,a}$	Number of APs in X lost by ice nucleation	kg^{-1}
Q	Passive clock tracer	kg^{-1}
Q_0	Value of Q outside of the cold cloud	kg^{-1}
Q_r	Raindrop's mass m. r.	kg kg^{-1}
t	Time	s
t^*	t since the start of the isothermal phase of the laboratory experiment (Jakobsson et al., 2022)	s
w	Vertical velocity of air	m s^{-1}
z	Height	m
α_X	Fraction of $n_{IN,1,*}$ ($H_X = 1$) from INP activity of AP from X	-
β	Exponent in power-law dependence of temperature shift on time	-
Ω_X	Total surface area of all APs of diameters larger than 0.1 μm from X (not depleted by ice nucleation while inside the cloud)	(aerosol) m^2 (air) kg^{-1}
$\Omega_{X,1,*}$	Background tropospheric component of Ω_X for $0.1 \geq D_X \geq 1$ μm	(aerosol) m^2 (air) kg^{-1}
$\Omega_{X,rain}$	Total surface area of all APs bigger than 0.1 μm in group X immersed in liquid raindrops	(aerosol) m^2 (air) kg^{-1}
Δt	Model time step	s
ΔT_X	Shift in T in time-dependent approach of INP freezing	K
μ_X	Average number of activated ice embryos per AP in group X	-
$\xi(T)$	The function that varies between 0 and 1 for $-5 < T < -2$ºC	-
τ_Q	Relaxation time scale	s
v_t	Fall speeds of raindrops in each size bin	m s^{-1}
RH	Relative Humidity w. r. t. (plane) water	%
RH_i	Relative Humidity w. r. t. ice	%
$\tilde{n}_{IN,X}$	Modified $n_{IN,X}$ representing time dependent INP activity	kg^{-1}
$\tilde{n}_{IN,rain}$	Modified $n_{IN,rain}$ representing time dependent INP activity	kg^{-1}

Abstract

The role of multiple groups of primary biological aerosol particles (PBAPs) as ice nucleating particles (INPs), and of ice formation processes such as time-dependent freezing of various INPs, and various secondary ice production (SIP) mechanisms in overall ice concentration has been evaluated in a range of cloud systems by simulating them numerically with the state-of-the-art ‘Aerosol-Cloud’ (AC) model in a 3D mesoscale domain. Also, the mechanisms of aerosol indirect effects (AIEs) arising from anthropogenic INPs, and the responses to these AIEs from time-dependent INP freezing and SIP processes are investigated in the simulated clouds. The cloud systems simulated with AC are: events of summertime deep convection observed over Oklahoma, USA during the Midlatitude Continental Convective Cloud Experiment (MC3E) in 2011 on 1) 11 May, and 2) 20 May, and wintertime 3) orographic clouds observed during the Atmospheric Radiation Measurement Cloud Aerosol Precipitation Experiment (ACAPEX) on 07 February 2015 over North California, and 4) supercooled layer clouds observed over Larkhill, UK, during the Aerosol Properties, Processes And Influences on the Earth’s climate (APPRAISE) campaign on 18 February 2009.

AC uses the dynamical core of the Weather Research and Forecasting (WRF) model, modified Geophysical Fluid Dynamic Laboratory (GFDL) radiation scheme, and hybrid bin-bulk microphysics scheme. AC is validated adequately with the coincident aircraft, ground-based, and satellite observations for all four cases. AC forms secondary ice through the Hallett-Mossop (HM) process of rime-splintering, and fragmentation during ice-ice collisions, raindrop freezing, and sublimation of dendritic snow and graupel. A measure of SIP is defined using the term ‘ice enhancement’ (IE) ratio which is the ratio between the number concentration of total ice particles and active INPs at cloud tops.

For both cases in MC3E, overall, PBAPs have little effect (+1-6%) on the cloud-liquid (droplet mean sizes, number concentrations, and their water contents) properties, overall ice concentration, and on precipitation. AC predicts the activity of various INPs with an empirical parameterization (EP). The EP is modified to represent the time-dependent approach of INP freezing in light of our published laboratory observations. It is predicted that the time dependence of INP freezing is not the main cause for continuous ice nucleation and precipitation in all simulated cases. Rather, the main mechanism of precipitation formation is the combination of various SIP mechanisms (in convection) and recirculation-reactivation of dust particles (in APPRAISE layer cloud episode). Also, for all cases, the inclusion of time dependence of INP freezing causes little increase (about 10-20%) in the total ice concentration and ice from all SIP.

Regarding SIP, in young developing convective clouds of MC3E (11 May), with tops > -15^{o}C, the initial explosive growth is from the fast HM process, creating IE ratios as high as 10^3. By contrast, in mature convective clouds (tops < -20^{o}C), fragmentation in ice-ice collisions prevails, creating IE ratios of up to about 10^2-10^3. Regarding AIEs from INPs, increasing anthropogenic pollution is predicted to exert a net cooling in APPRAISE, and a strong net warming in MC3E (11 May). Furthermore, these net AIEs are mainly from glaciated clouds. Overall, the contribution to the AIEs from ice formation processes, such as time-dependent INP freezing and SIP, shows a high sensitivity with respect to anthropogenic INPs (about 20-60% increase in net AIEs).

Also, two new indirect effects associated with ice initiation mechanisms are proposed here. These are, 1) the 'SIP' indirect effect, and 2) the 'time-dependent INP' indirect effect. It is predicted that in APPRAISE and MC3E, both SIP and time-dependent INP indirect effects form less than 30%, and more than 50% of the net AIE, respectively.

1. Introduction

1.1 Importance of Clouds: Weather and Climate Perspective

Clouds are one of the influential manifestations of nature. A cloud is composed of hydrometeors that can exist in either the liquid or solid (ice) phase. Cloud hydrometeors form when water vapor condenses on the aerosol particles (APs). APs are small particles (diameters between 0.5 nm and 10 µm) suspended in the atmosphere such as ammonium sulfate, sea salt, black carbon (soot), soluble and insoluble organics, and biological particles (Lohmann et al., 2016; Warneck, 1999). Clouds can be observed in different sizes and shapes. There are different types of clouds, namely, 1) cirrus clouds which are generally composed of ice-crystals and have a feathery, hair-like appearance at high altitudes, 2) cumulus clouds, appearing as fluffy, cauliflower-shaped formations occasionally associated with precipitation, 3) nimbostratus clouds which are low or mid-level rain-bearing clouds characterized by their dark or grey appearance.

Clouds and the associated rainfall are the most important yet least understood components of the climate system (Boucher et al., 2013). Clouds cover about half of the globe (Flossmann, 1998; Liou, 2002; Boucher et al., 2013; King et al. 2013) and are considered one of the most crucial elements of Earth's energy budget, reflecting about 15% of the incident solar radiation to space (Boucher et al., 2013). Clouds control the amount of incoming shortwave (SW) and outgoing longwave (LW) radiation, thereby regulating the earth's temperature, driving the global hydrological cycle, and serving as a source/sink for atmospheric pollutants through precipitation (Hartmann et al., 1992; Flossmann, 1998; Houghton et al., 2001; Ramanathan et al., 2001; Lohmann, 2006; Boucher et al., 2013; Ervens, 2015; Kudzotsa et al., 2016; Ryu and Min, 2022).

Cloud formation in the atmosphere occurs when an air parcel becomes saturated with respect to water/ice. This typically takes place during the ascent of the air parcel caused by various mechanisms. These mechanisms are:

1) *Orographic lifting,*
2) *lifting along frontal boundaries,*
3) *surface-air convergence, and*
4) *surface heating and free convection.*

Also, depending on the presence of hydrometeors and their top temperature, clouds can be classified as:

i. *liquid* clouds are characterized by warmer tops (> 0ºC) and consists of only liquid particles. These clouds are also known as *warm* clouds.

ii. *Mixed-phase* clouds consist of both liquid and ice particles and their tops can extend up to the −36ºC level, and

iii. *Ice-only* clouds form at levels colder than the −36ºC and consist of only ice particles. They can also form at temperatures as warm as 0ºC, provided that the ascent is weak enough (e.g., Westbrook and Illingworth, 2013 [hereafter 'WI13']).

Initiation of cloud hydrometeors occurs through processes known as *homogeneous* and *heterogeneous* nucleation. However, the homogeneous nucleation of cloud droplets from vapor is not feasible, as the supersaturation with respect to liquid water (s_w) usually does not exceed 10% (Lohmann et al., 2016). By contrast, heterogeneous nucleation of cloud droplets occurs at levels warmer than the −36ºC and in the presence of soluble aerosol particles (diameters about 1 µm) such as ammonium sulfate, sea salt, and soluble organics, depending on s_w. These APs are referred to as cloud condensation nuclei (CCN) (Rogers and Yau, 1996; Lohmann et al., 2016; Flossmann et al., 2018). Typically, CCN concentrations over continents and oceans are on the order of about 10^3 and 10^2 cm^{-3}, respectively (Hobbs and Radke, 1969; Pruppacher and Klett, 1997).

Once a cloud grows above the freezing level (< 0ºC), it may contain both cloud droplets and ice crystals. Mechanisms of ice initiation are fundamental for the climate, as most of the global precipitation is chiefly associated with the ice phase (Lau and Wu, 2003; Lohmann, 2006; Field and Heymsfield 2015). Yet, these mechanisms are uncertain (Cantrell and Heymsfield, 2005; Field et al., 2017). The initiation of ice crystals in the clouds at subzero levels is described below.

1.1.1 Ice Initiation in Clouds

Two phase transitions can initiate ice at subzero levels (Rogers and Yau, 1996; Pruppacher and Klett, 1997). These are briefly described here.

1.1.1.1 Homogeneous Ice Nucleation

In *homogeneous* nucleation (Fig. 1a), an ice crystal forms from the freezing of supercooled liquid droplets without any aerosol activity under sufficiently high supersaturation with respect to ice (s_i) (Rogers and Yau, 1996; Pruppacher and Klett, 1997; Murray et al., 2010). Homogeneous ice nucleation occurs at levels colder than $-36^{o}C$, where a chance collision of vapor molecules leads to the formation of a stable ice embryo. An ice crystal can be formed homogeneously through two types.

The first type involves ice initiation through the spontaneous freezing of supercooled cloud drops/raindrops, and APs at temperatures colder than $-36^{o}C$, depending on droplet size. The second type of homogeneous ice nucleation is the homogeneous freezing of solution droplets, which occurs at colder temperatures as soon as s_i exceeds the critical supersaturation (Koop et al., 2000; Phillips et al., 2007). Homogeneous freezing of cloud droplets/raindrops and solution droplets mainly occurs in deep convective and cirrus clouds, respectively.

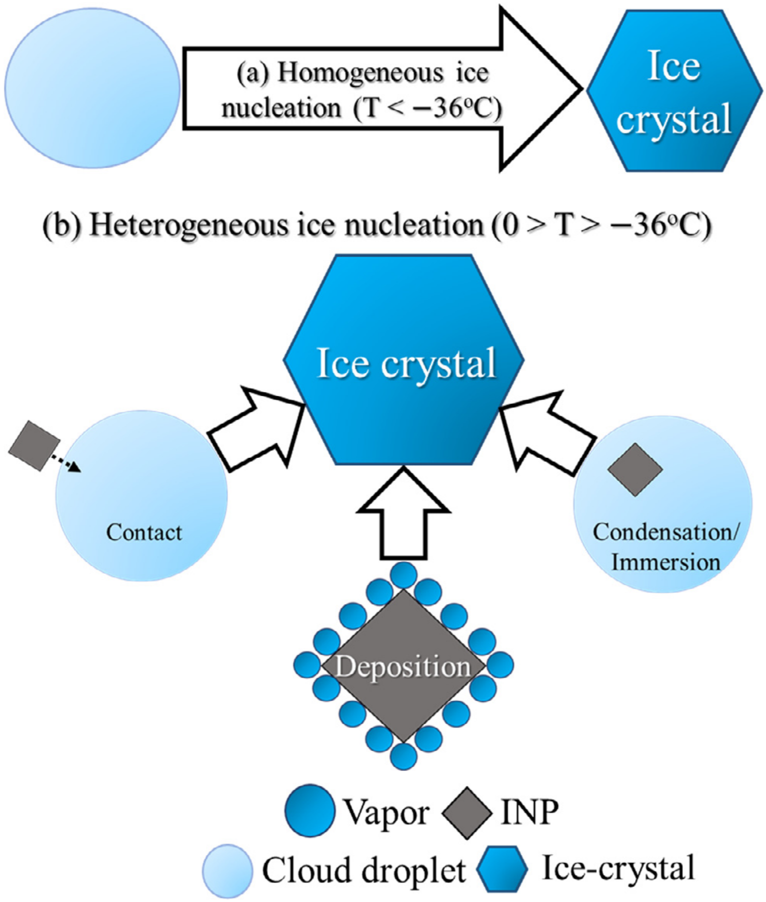

Figure 1. Schematic representation of (a) the homogeneous and (b) various modes of heterogeneous ice nucleation processes.

1.1.1.2 Heterogeneous Ice Nucleation

Heterogeneous ice nucleation involves the formation of an ice crystal due to the activity of solid APs at subzero levels (DeMott, 1990; Rogers and Yau, 1996; Phillips et al., 2008; Murray et al., 2010, 2012; Kanji et al., 2017). These solid APs are commonly referred to as ice nucleating particles (INPs) and are relatively rare in the atmosphere, with typical concentrations between 10^{-5} and 1 L^{-1} at temperatures near −10°C (DeMott et al., 2003; Lasher-Trapp et al., 2016). Active sites on the surface of such INPs are required for ice nucleation to occur at temperatures warmer than −36°C. They are scarce and efficiently absorb water molecules, thus reducing the energy barrier for the formation of ice embryos.

There is a wide variety of sources of INPs in the atmosphere, both natural and anthropogenic. Natural sources include deserts, oceans, volcanic eruptions, and the emission of vegetation debris. Similarly, anthropogenic sources are biomass burning, deforestation, and industrial activities (Kanji et al., 2017). A range of solid APs originating from these sources such as dust (mineral and soil), insoluble organics, soot, and primary biological aerosol particles (PBAPs), which include pollen, bacteria, detritus, algae, fungi, and plant fragments, phytoplankton, lichens may initiate primary ice by acting as INPs (Hobbs and Locatelli, 1969; DeMott, 1990; Phillips et al., 2009, 2013; Kanji et al., 2017; Flossmann et al., 2018; Patade et al., 2021). The chemical composition and concentrations of INPs vary significantly across the globe, and they can significantly alter the microphysical and radiative properties of clouds (Phillips et al., 2003; Cantrell and Heymsfield, 2005; Lohmann 2006; Kudzotsa et al., 2016).

Various heterogeneous nucleation processes (Fig. 1b) can lead to the formation of the first ice crystal above the freezing level (Vali, 1985; DeMott et al., 1983; Pruppacher and Klett, 1997; Lohmann, 2006). These processes include:

i. *Deposition ice nucleation* (Fig. 1b) occurs in an environment supersaturated with respect to ice. In this mode of ice nucleation, water vapor taken up by the INP surfaces can directly transform into an ice phase without any intermediate liquid phase (Kanji et al., 2017). This requires a relative humidity with respect to ice (RH_i) exceeding 100% in the ambient air. Deposition nucleation could be significant in high-level clouds (e.g., cirrus) (Cziczo et al., 2013). However, in mixed-phase clouds, this mode of ice nucleation is less significant as the INPs are first expected to be activated as cloud droplets (Ansmann et al., 2008; Field et al., 2006).

ii. *Contact freezing* in which the ice particle forms upon contact between an active INP and a supercooled droplet (Fig. 1b). There are two ways by which the ice can be nucleated through contact freezing, 1) 'outside-in' in which the INP outside of the droplet collides with it, and 2) the freezing of a droplet occurs when a pre-existing INP touches the droplet surface from within the droplet (Shaw et al., 2005; Fornea et al., 2009).

iii. *Condensation/Immersion freezing* involves an INP becoming immersed in a cloud droplet, typically at warmer temperatures (> 0ºC), and then initiating the ice phase once the droplet reaches subzero levels (Fig. 1b).

In mixed-phase clouds, heterogeneous ice nucleation mainly occurs through deposition, condensation, and immersion freezing while contact nucleation makes a minimal contribution to the total heterogeneous ice formed (Phillips et al., 2007; Ansmann et al., 2008; WI13).

The ice nucleation ability of all INPs varies significantly depending on their type and concentration in the environment. Mineral dust is generally considered the most important type of INP, and its ice nucleation onset can occur at subzero temperatures as warm as −10ºC (Hoose and Möhler, 2012; Phillips et al., 2013; Kanji et al., 2017). Furthermore, the activity of dust INPs increases with increasing surface area (Phillips et al., 2008; Kanji et al., 2017).

PBAPs, emitted from land vegetation and oceans (Després et al., 2012), initiate ice at temperatures as warm as −2ºC (Patade et al., 2021). Additionally, incomplete combustion of fossil fuels can produce soot, which can also play an important role in ice formation. However, it has been argued that soot is not a significant contributor to heterogeneous ice formation, especially from freshly emitted fossil fuel combustion (Koehler et al., 2009; Bond et al., 2013). Moreover, a modelling study by Schill et al. (2020) demonstrated that soot, from biomass burning, is a minor contributor to INP on the global scale. By contrast, a strong correlation was observed between soot concentrations and in-cloud ice concentrations for thin wave clouds over Wyoming, which were affected by biomass burning (Twohy et al., 2010).

Several previous studies have proposed that the heterogeneous ice nucleation can be: 1) time-independent and, 2) time-dependent in nature (Levine, 1950; Langham and Mason, 1958; Vali and Stansbury, 1966; Vonnegut and Baldwin, 1984; Vali, 1994, 2008; Jakobsson et al., 2022 [hereafter 'JK22']). These are described below.

Time Independent Heterogeneous Ice Nucleation

The time-independent approach of INP activation assumes that ice nucleation is an instantaneous process and occurs at deterministic temperatures at specific 'active' sites (Vali 1994, 2008), resulting in identical INPs nucleating all together. These active sites are characterized by the lowest particle-ice interfacial energy and hence activation takes place at higher temperatures almost instantaneously (Niedermeier et al., 2011). Under isothermal conditions, this hypothesis assumes no time dependence, and any INP activation occurs at the onset of the nucleation (Chen et al., 2008).

Time Dependent Heterogeneous Ice Nucleation

At levels warmer than −36ºC, the drops may contain different types of impurities (APs), and the freezing probability of such drops may vary (Vali and Stansbury, 1966), as later observed experimentally by (Vonnegut and Baldwin, 1984). At a given temperature the freezing probability depends on the surface area of the INP and the time for which an INP remains in the favorable environment (Chen et al., 2008; Murray et al., 2012).

Welti et al. (2012) observed that the immersion freezing mode of INP activation exhibits time dependence, which is the basis for WI13 to propose the time dependence of INP freezing being the main source for continuous ice nucleation and precipitation in supercooled stratiform clouds. However, their hypothesis was not supported by any modelling evidence, and the relative importance of the time dependence of INP freezing is not yet well understood. Vali (2014) assessed various laboratory studies and concluded that the time-dependent approach of INP freezing is less important and it can be neglected from numerical models, especially for systems with high cooling rates (about 1-2 K min^{-1}) corresponding to ascent speeds up to about 3 m s^{-1} (Kanji et al., 2017). Nevertheless, this was not conclusively verified with modelling simulations.

1.1.2 Ice Multiplication in Clouds

Previous aircraft studies of natural convective clouds with tops warmer than −36ºC (Mossop, 1985; Hobbs et al., 1980; Harris-Hobbs and Cooper, 1987; Cantrell and Heymsfield, 2005) have observed that the number concentrations of ice particles often exceed the number concentrations of INPs by about 10^2 to 10^4 orders of magnitude. It is further observed that the discrepancy in the observed number concentrations of INPs and ice particles remains (Ladino et al., 2017) even with the processing algorithms (Field et al., 2006) and modified optical probes (Korolev et al., 2011) that eliminates possible biases caused by artificial shattering (Field et al., 2017).

Therefore, it has long been proposed that, following initial primary ice nucleation, some mechanisms must exist at subzero temperatures (> −36ºC) that can enhance the number concentrations of ice particles. These mechanisms are known as ice multiplication or secondary ice production (SIP) mechanisms (Hobbs, 1969; Hallett and Mossop, 1974 [hereafter 'HM']; Vardiman, 1978; Oraltay and Hallett, 1989; Takahashi et al., 1995; Lohmann et al., 2016; Phillips et al., 2017a; Miltenberger et al., 2020, 2021; Deshmukh et al., 2022). SIP processes form new ice particles in the presence of pre-existing (primary) ice without requiring the activity of INPs (or homogeneous freezing) (Field et al., 2017) under suitable conditions. Furthermore, the SIP processes must involve precipitation, since wave clouds (e.g., Eidhammer et al., 2010) and layer clouds (WI13) too thin to precipitate are seen to have little ice enhancement.

The degree of enhancement in the number concentrations of ice particles due to ice multiplication can be defined using the term called '*ice enhancement*' (IE) ratio. This ratio represents the average number concentrations of ice particles to the number concentrations of active INPs at any in-cloud level (Hobbs et al., 1980; Pruppacher and Klett, 1997). There is a range of possible SIP processes proposed so far that depends on temperature, vertical velocity, and particle size distributions, these are:

1.1.2.1 The Hallett-Mossop process of Rime-splintering

The HM process of rime-splintering is an important ice multiplication process in mixed-phase clouds and is the most studied SIP process among all SIP mechanisms known so far. HM (1974) observed that during the riming of supercooled cloud drops (diameters > 24 μm), numerous ice splinters break away for temperatures between −3 and −8°C. The rate of splinter production during riming of a supercooled drop is maximum at about −5°C and for an updraft speed of about 2.7 m s^{-1} (HM 1974, their Fig. 2).

The HM process is temperature-dependent because at subzero temperatures warmer than −3°C, supercooled droplets do not form an ice shell while at temperatures colder than −8°C, ice particle growth becomes rapid and hence the internal pressure is not sufficient to break the ice shells (Griggs and Choularton 1983; Mason 1996). According to the theory proposed by Griggs and Choularton (1983), between −3 and −8°C, pressure built up inside the freezing droplet during its accretion on a large ice particle. This pressure is later released by a crack in the outer frozen shell, releasing an unfrozen freezing liquid that eventually freezes and forms secondary ice.

The HM process is widely studied, evident with both observational and experimental (Harris-Hobbs and Cooper, 1987; Blyth and Latham 1993; Rangno and Hobbs 2001; Crosier et al., 2011 [hereafter 'C11']; Heymsfield and Willys 2014; Patade et al., 2016) and modelling studies (Phillips et al., 2003, 2005; Huang et al., 2017; Miltenberger et al., 2020, 2021; Lasher-Trapp et al., 2021; Gayatri et al., 2022; Waman et al., 2022, 2023a [hereafter 'Wa22' and 'Wa23a']) (Fig. 2). Furthermore, several numerical modelling studies have shown that the HM process and raindrop freezing fragmentation (Sec. 1.1.2.3) dominates the overall ice concentrations typically in young convective clouds with tops warmer than −20°C, creating IE ratios as high as 10^3 (Wa22; Wa23a) in such clouds. However, a recent laboratory study by Hartmann et al. (2023) found no substantial activity of SIP via the HM process.

Apart from the HM process, many alternative ice multiplication mechanisms must exist in clouds that can cause explosive growth of ice crystal concentrations, typically at levels colder than −8°C. These mechanisms are discussed below.

1.1.2.2 Fragmentation during Ice-Ice Collisions

Langmuir (1948) proposed that SIP may occur during the collision between ice particles. This hypothesis was later verified by several field and laboratory studies (Hobbs and Farber 1972; Vardiman 1978; Takahashi et al., 1995, reviewed by Phillips et al., 2017a, b). Production of ice-crystal splinters during ice-ice collisions depends on ambient temperature with a maximum at about −15°C (Takahashi et al., 1995). This can be mainly attributed to the formation of fragile, vapor-grown branches on rimed ice particles in the dendritic regimes.

Fragmentation in ice-ice collisions was also studied theoretically by Hobbs and Farber (1972), Yano and Phillips (2011), Yano et al. (2016), and Phillips et al. (2017a, b). A theoretical formulation proposed by Phillips et al. (2017a) is based on the principle of energy conservation. The formation of secondary fragments during ice-ice collisions depends on the sizes and relative fall velocities of the colliding ice particles, ambient temperature, and riming intensity of ice particles (Korolev and Leisner 2020). Several modelling studies (Fridlind et al., 2017; Sotiropoulou et al., 2021; Zhao et al., 2021; Patade et al., 2022; Wa22; Wa23a) found that fragmentation in ice-ice collisions is a prolific SIP mechanism in the simulated cloud systems (Fig. 2).

The HM process is predicted to prevail in relatively young clouds (tops warmer than −15°C). By contrast, fragmentation in ice-ice collisions prevails at longer times in clouds causing an explosive growth of ice crystal numbers (IE ratios ~ 10^3-10^4) in their mature stage (Yano and Phillips, 2011; Wa22; Wa23a).

1.1.2.3 Fragmentation during Raindrop Freezing

SIP may also occur during the shattering of freezing drizzle or raindrops. Several laboratory studies (Johanson and Hallett 1968; Takahashi and Yamashita 1969, 1970; Pruppacher and Schlamp 1975; Leisner et al., 2014; Wildeman et al., 2017; Keinert et al., 2020) and aircraft observations (Rangno 2008; Lawson et al., 2015; Korolev et al., 2020) have observed fragmentation during droplet freezing (Fig. 2). During raindrop freezing, liquid may get trapped inside an ice shell which may break once the excess pressure built up during freezing exceeds the threshold value, emitting spikes and fragments of secondary ice.

Based on published laboratory observations of drops in free-fall, Phillips et al. (2018) proposed an empirical formulation of SIP during raindrop freezing. They proposed two modes of fragmentation during raindrop freezing. The first mode involves fragmentation during freezing of spherical (0.05-5 mm) drizzles or raindrops. In this mode, the collision of a supercooled drop with a less massive ice particle initiates quasi-spherical freezing of a drop, which can also be seen during the heterogeneous freezing of raindrops (due to immersed INP). During freezing, the outer ice shell may eventually break, generating fragments of secondary ice. The second mode involves non-spherical freezing when a supercooled raindrop collides with a more massive ice particle, which emits a secondary splash of droplets that eventually freeze to form secondary ice (Phillips et al., 2018; James et al., 2021). Fragmentation during raindrop freezing depends on the ambient temperature and the sizes of colliding hydrometeors.

1.1.2.4 Fragmentation during Sublimation

Another possible source of SIP is fragmentation during the sublimation of ice particles, such as dendritic snow and graupel, in subsaturated cloudy regions, as evident in laboratory studies (Fig. 2) by Oraltay and Hallett (1989), Dong et al. (1994), and Bacon et al. (1998) (Table 1). Oraltay and Hallett (1989) observed that the dendritic ice crystal partially sublimates and generates secondary ice splinters when RH_i is below 70%. These laboratory studies were the basis for Deshmukh et al. (2022) to propose a formulation for fragmentation during the sublimation of dendritic snow and graupel.

Fragmentation during sublimation depends upon particle size and shape, fall velocity, ambient air temperature, and RH_i (Deshmukh et al., 2022) and can be significant in deep convective descents ($w < -2$ m s^{-1}) (Deshmukh et al., 2022; Wa22) creating IE ratios of about 10.

Table 1. Summary of the laboratory studies of SIP during sublimation of ice particles.

Study	T (ºC)	RH_i (%)	Ventilation speed (m s^{-1})	Particle habits
Oraltay and Hallett 1989	-17 to -15	<70	0.1 to 0.2	Dendrites
Dong et al., 1994	-18 to -5	50 to 90	about 1	Rimed ice and needles
Bacon et al., 1998	-30 to 0	85 to 100	-	All ice particles

Apart from these four processes (Sec. 1.1.2) of SIP, two more ice multiplication mechanisms were proposed (Korolev and Leisner, 2020) that are thought to produce secondary ice in clouds. These are,

i. the activation of pre-existing INPs in the transient supersaturation of falling droplets (Chouippe et al., 2019; Prabhakaran et al., 2019, 2020), and

ii. fragmentation due to thermal shock at the droplet-ice particle interface cause to the release of latent heat during droplet freezing (Dye and Hobbs 1968). The breakup of an ice crystal may also occur without any change in the freezing drop or when the drop is cracked.

Regarding (i), there are reasons to doubt it being prolific, since as soon as the humidity goes well above water saturation any solid INP activates as a cloud droplet, with any subsequent freezing being temperature-dependent and independent of ambient humidity. Arguably regarding (ii), this mechanism is already active in observed raindrop-freezing in lab experiments of drops in free-fall, since many of these used a cloud of ice crystals in the cloud chamber to induce freezing by collision with the supercooled drops. Hence it is already treated in the scheme by Phillips et al. (2018).

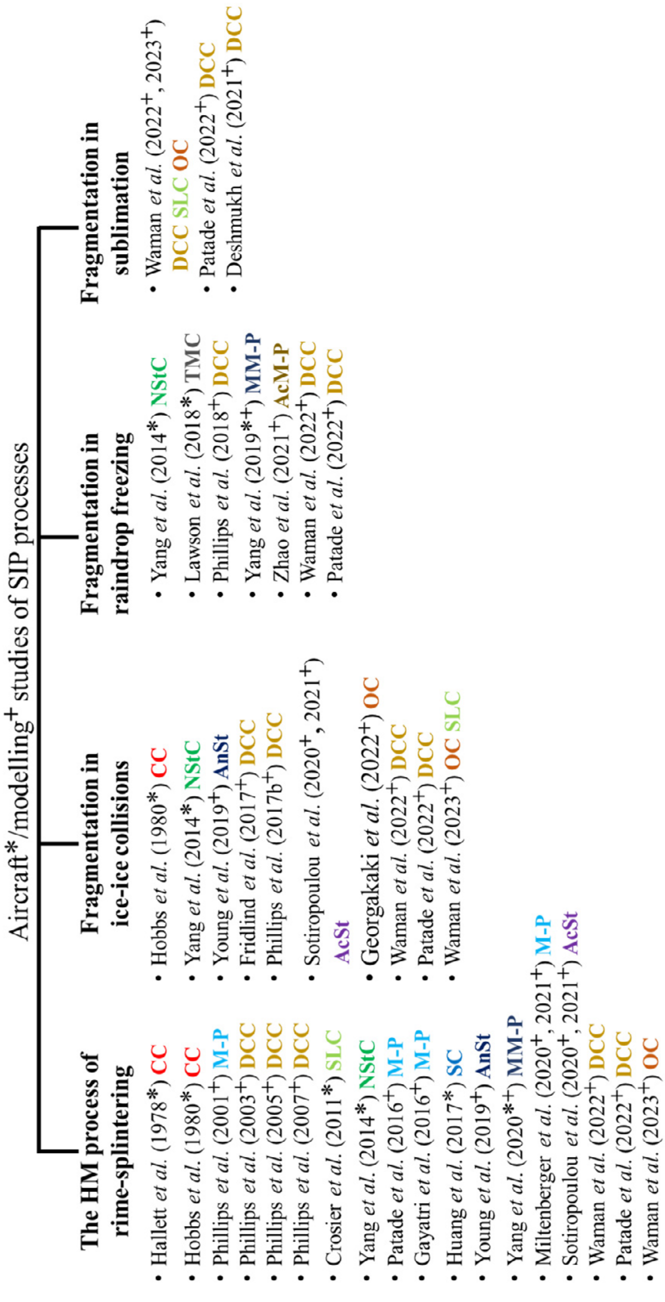

Figure 2. Flowchart showing the aircraft (asterisks) and modelling (plus) evidence of SIP processes active in various cloud systems such as convective clouds (**CC**), supercooled layer clouds (**SLC**), nimbostratus clouds (**NStC**), mixed-phase clouds (**M-P**), shallow cumulus (**SC**), Antarctic stratocumulus (**AnSt**), Arctic stratocumulus (**AcSt**), deep convective clouds (**DCC**), orographic clouds (**OC**), tropical marine cumulus (**TMC**), maritime mixed-phase (**MM-P**), and Arctic mixed-phase clouds (**AcM-P**).

Figure 2 summarizes aircraft and modeling evidence of SIP processes that are found to be active in different cloud systems.

1.1.3 Processes of Precipitation Formation

The microphysical processes of clouds can greatly affect precipitation (Takahashi and Kawano 1998; Grabowski et al., 1999) which is an important component of the global hydrological cycle (Field and Heymsfield 2015). Precipitation formation mainly occurs through two distinct processes (Rogers and Yau 1996; Rauber et al., 2000). These are, 1) the *warm rain*, and 2) the *ice crystal* process. Both of these processes can co-exist and are briefly described here.

1.1.3.1 Warm-rain (Collision-Coalescence) Process

Once nucleated, a droplet can grow by diffusion of water molecules from the vapor onto its surface, which can only grow cloud droplets up to a few micrometers in size (Rogers and Yau, 1996). Hence, condensation alone cannot grow cloud droplets to a precipitable size. The mechanism responsible for precipitation formation in warm clouds is known as the *collision-coalescence*, or *warm-rain* process (Gao et al., 2021). In this process, cloud droplets of different sizes collide and stick together and form larger drops of precipitation size which may fall with higher terminal velocity collecting more and more cloud droplets serving positive feedback of collision-coalescence whereas droplet breakup limits the growth of droplets.

Typically, a warm-based cloud (> 10ºC) of about 2-3 km depth has sufficient updrafts, liquid water, and a lifetime to sustain collision-coalescence growth. The warm rain process occurs in both shallow and deep convective clouds. In thunderstorm and mesoscale convective systems (MCS), the warm rain process is the source of condensed water (cloud droplets) to precipitable water (drizzle and raindrops) (Gao et al., 2021). The warm-rain process can be significant in tropics and subtropics for shallow clouds (Lau and Wu, 2003; Field and Heymsfield 2015) and is greatly affected by loadings and properties of APs (Dagan et al., 2015).

1.1.3.2 Ice crystal Process

Another mode of precipitation formation associated with cold clouds is the '*ice crystal*' process in which ice crystals formed during nucleation grow to form snow following vapor diffusion or aggregation. Aggregation involves the collection of ice crystals. It is dominant at dendritic levels (−12 to −17ºC), where particles are stickiest (Rogers and Yau, 1996; Phillips et al., 2015). Snow formed during vapor diffusion or aggregation may rime to form graupel which may subsequently melt to form 'cold' rain (Rogers and Yau 1996). Prolonged riming of ice crystals can result in hail formation. The ice crystal process of precipitation can significantly contribute to surface precipitation globally (Field and Heymsfield 2015), especially in the tropics and midlatitudes (Lau and Wu 2003).

Furthermore, in mixed-phase clouds, snow may form through the Bergeron-Findeisen process. This is a special type of ice crystal process involving the evaporation of supercooled cloud liquid and is chiefly active in mixed-phase clouds, where supercooled liquid and ice coexist. In such clouds, saturation vapor pressure over supercooled liquid is higher than that over ice. This variation in saturation vapor pressures between liquid and ice leads to the growth of ice crystals at the expense of supercooled droplets.

Figure 3 shows a schematic of a convective cloud in its mature stage (top colder than -36^{o}C), summarizing the microphysical processes described in Sec. 1.1.1-1.1.3. It shows the droplet activation through heterogeneous nucleation of soluble APs at levels near cloud-base, heterogeneous (0 to -36^{o}C) and homogeneous ice nucleation ($< -36^{o}$C), possible SIP processes, and the warm rain and ice crystal processes of precipitation formation active in such convective clouds.

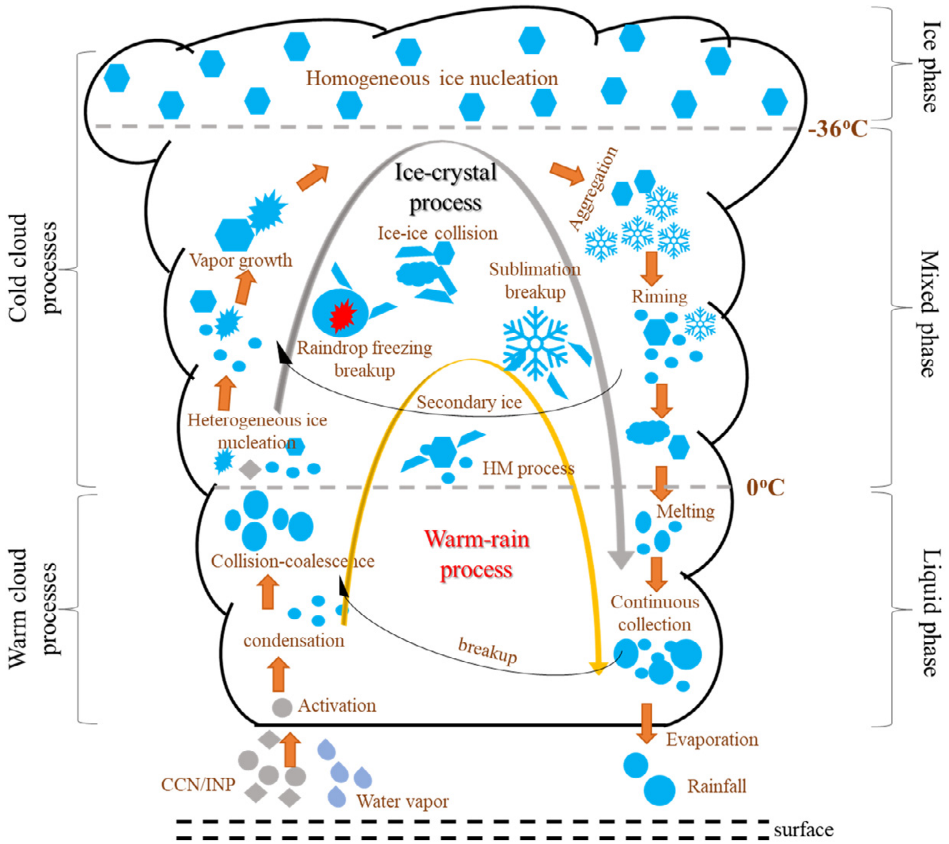

Figure 3. Schematic of a deep convective cloud with its top reaching well above the −36°C level (mature stage) illustrating initiation of cloud hydrometeors, warm rain and ice crystal process of precipitation formation, and mechanisms of SIP.

1.1.4 Radiative Importance of Aerosols and Clouds

Clouds can enhance the planetary albedo by reflecting the incoming SW radiation. Also, they can exert a greenhouse effect by trapping outgoing LW radiation. The net effect of these SW and LW components of radiation is known as the cloud radiative effect (CRE). On the global scale, at the top of the atmosphere (TOA), by enhancing the planetary albedo, clouds exert an annual SW CRE of about −50 W m^{-2} (Boucher et al., 2013). Also, clouds exert a net annual LW CRE of about +30 W m^{-2} (Boucher et al., 2013). Hence, on the global scale, clouds cause a net cooling of the present-day climate system (Yli-Juuti et al. 2021), with an effective CRE of about −20 W m^{-2}. However, the SW and LW CRE depend on the altitude, type, and optical properties of the clouds. For example, high-level clouds (e.g., cirriform) emit less outgoing LW radiation to space because they are colder than the mean emitting level of the troposphere, thus exerting a strong greenhouse warming of the surface. It arises from the strong dependency of the emitted radiative flux on temperature by the Stefan-Boltzmann law (Liou, 2002). Also, such high-level clouds cause a cooling or warming, depending on whether they are thin or thick. Optically thick mid-level clouds can cause either a warming or a cooling (Sotiropoulou et al., 2021).

The global anthropogenic aerosol loading has significantly increased in the present day compared to pre-industrial times (Haywood and Boucher, 2000; Lohmann and Fiechter, 2005; Takemura, 2012) and is considered an important driver of climate forcing (Boucher et al., 2013). Anthropogenic APs can greatly influence the radiative budget of Earth's atmosphere through direct reflection/absorption of incoming SW and emission/absorption of outgoing LW radiations, known as the *direct effect*.

In their *indirect effect*, APs can modify the radiative impacts of clouds on Earth's radiation budget by altering their microphysical, macrophysical, and hence radiative properties (Twomey, 1974; Flossmann, 1998; Haywood and Boucher, 2000; Penner et al., 2004; Cantrell and Heymsfield, 2005; Gettleman et al., 2012; Wang et al., 2014; Kudzotsa et al., 2016; Wa22). A case study by Romakkaniemi et al. (2012) over Germany has shown that in polluted conditions, aerosol indirect effects (AIEs) dominate, whereas locally, their direct effects are more significant. The change in net radiative flux at the TOA due to changes in APs loading is defined using the term called *radiative forcing* (Kudzotsa et al., 2016; Lohmann, 2006).

In its first indirect effect, known as the *cloud albedo-emissivity effect* (Twomey effect) (Twomey, 1974; Charlson et al., 1992; Lohmann and Lesins, 2002; Lohmann, 2006; Boucher et al., 2013; Kudzotsa et al., 2016b), APs can alter the cloud microphysical structure by acting as CCN or INPs, thereby changing their reflective properties and influencing cloud albedo. Anthropogenic activity can also modify the lifetime of the cloud through precipitation efficiency, affecting its 3D extent. This associated aerosol indirect effect is known as the *lifetime effect* (Albrecht, 1989; Lohmann, 2006; Kudzotsa et al., 2016).

High aerosol loading in Earth's troposphere leads to an increased number of cloud hydrometeors of smaller sizes, resulting in greater reflection of incoming SW radiation and causing net cooling (Lohmann and Feichter, 2005; Christensen et al., 2016). APs can absorb incident radiation, resulting in net heating which may increase the evaporation of cloud hydrometeors, known as the *semi-direct effect* of aerosols (Lohmann and Fiechter, 2001; Johnson et al., 2004; Hill and Dobbie, 2008; Koch and Genio, 2010).

Previous modelling studies (Young et al., 2019; Miltenberger et al., 2021; Wa22) have shown that SIP can affect the radiative properties of clouds by modifying their microphysical and macrophysical structure. Increased SIP activity enhances cloud glaciation rate, thereby reducing cloud cover (Phillips et al., 2017a; Wa22; Wa23b) allowing more solar radiation to reach the earth's surface.

1.2 Importance of Cloud-Resolving Models

The significance of clouds extends beyond their impact on the hydrological cycle or their interaction with radiation. In fact, clouds play a crucial role by releasing latent heat during phase transitions, emerging as a dominant source of energy for atmospheric motions that span over a few mm to thousands of kilometers. Clouds, along with the microphysical, dynamical, and radiative processes associated with them, can occur over a few tens to a few hundred kilometers. Cloud-Resolving models (CRMs) are the state-of-the-art tool to study clouds and associated processes due to their ability to simulate clouds at finer spatial (about a few km) and temporal (about a few seconds) scales. Some important features of CRMs are.

i. CRMs explicitly resolve individual clouds and their microphysical processes that allow a more accurate and realistic representation of the processes such as cloud formation, growth, and dissipation. These processes are crucial for understanding precipitation patterns and CRE.

ii. CRMs allow simulations of small-scale (e.g., single clouds) as well as large-scale (thunderstorm and squall lines) processes with a spatial resolution finer than about 2-3 km (Khain and Pinsky 2018).

iii. These models can explicitly resolve cloud-scale processes and hence an efficient tool to provide better forecasts of short-term weather events.

iv. CRMs provide a more accurate representation of the microphysical processes of the clouds, and their interaction with aerosols and radiation, hence are a powerful tool in atmospheric and climate research.

However, cloud processes remain as one of the largest sources of uncertainties in numerical weather and climate models (Boucher et al., 2013). These uncertainties may arise either from the complete absence or a lack of accurate representation of the cloud microphysical processes. The present study, using the state-of-the-art numerical model, closes the knowledge gaps related to the following aspects:

i. Importance of various biological particles in initiating ice.

ii. The role of time dependence of INP freezing in overall ice formation and precipitation.

iii. Evolution of various ice multiplication processes with clouds.

iv. How anthropogenically increased solid APs influence the cloud radiative properties.

The present work addressed a range of research questions, associated with the ice phase of the clouds, using a CRM model. These include the elucidation of the role of 1) various PBAPs, 2) time-dependent INP freezing in initiating the overall ice, and 3) the relative importance of various SIP mechanisms in different stages of the convective clouds, and 4) effects from solid aerosol pollution on the radiative properties of the simulated clouds. The present study also evaluates the impact from ice formation processes such as SIP and time-dependent INP freezing on the net AIEs, in the simulated clouds. Also, two new indirect effects, associated with these ice formation processes, are proposed here. These are, 1) the 'SIP' indirect effect, and 2) the 'time-dependent INP' indirect effect.

The structure of the thesis is as follows. Sections 2 and 3 describe the proposed research questions and hypotheses, Sec. 4 provides details of the numerical model used, as well as the cases of storms. Section 5 describes the case setup, and modifications made in the numerical model, along with various sensitivity tests performed. Section 6 summarizes the results and conclusions. Finally, Sec. 7 describes the key findings.

2. Scientific Hypotheses and Research Questions

As discussed in Sec. 1, the ice phase in clouds greatly controls precipitation and hence the hydrological cycle and water availability. Also, the interaction between radiation and ice particles can affect climate patterns and temperature distributions by changing the energy balance of the Earth-atmosphere system. Ice particles can also affect the microphysical properties of cloud hydrometeors by altering their sizes, water contents, and number concentrations as well as cloud optical properties by controlling the rates of the processes such as vapor growth, accretion, aggregation, riming, and ice multiplication. Furthermore, the ice phase can significantly alter the cover, age, and lifetime of the clouds through precipitation formation.

Hence, the overarching goal of the present study is to elucidate the fundamental processes and mechanisms that govern the formation and evolution of ice phase in clouds, including both primary and secondary ice production using the Weather Research and Forecasting (WRF) based Aerosol-Cloud (AC) model, which is a state-of-the-art CRM with a 3D mesoscale domain. Furthermore, the indirect effects of various solid aerosols via glaciated clouds have also been studied. Moreover, the present study also investigates the impact on the simulated indirect effects from ice formation processes such as time dependence of INP freezing and SIP.

The research questions and hypotheses of the present study are as follows.

A. How important are various species of PBAPs in initiating ice, controlling precipitation, and altering the microphysical structure of the simulated continental convective storm?

   Hypotheses:

   i. PBAPs can be one of the significant types of INPs and can greatly alter the cloud properties such as mass and number concentrations of ice particles.

   ii. PBAPs can significantly alter precipitation efficiency and radiative properties of the clouds.

B. Is the time dependence of INP freezing the main source for continuous ice nucleation and precipitation in a range of cloud systems?

Hypotheses:

i. Time dependence of INP freezing is the main cause for the observed ice concentrations in a range of cloud systems simulated numerically.

ii. Time dependence of INP freezing is the main mechanism for continuous ice nucleation and precipitation in the simulated cloud systems.

C. How are SIP mechanisms dependent on cloud-top temperature in a continental convective storm? How do various SIP processes differ in relative importance during the evolution of convective clouds?

Hypotheses:

i. Various SIP processes can form the observed ice particle number concentrations in the simulated clouds.

ii. The evolution of various SIP processes is dependent on the time and cloud-top temperature in the simulated clouds.

iii. The aircraft observed classic dependency of the IE ratio is dependent on cloud top temperature.

D. How do anthropogenically increasing solid APs affect the micro-, macrophysical and radiative properties of the simulated clouds compared pre-industrially? Can time dependence of INP freezing and SIP cause any impact on the predicted indirect effects from solid aerosols?

Hypotheses:

i. Anthropogenically induced INPs can significantly alter the micro- and macrophysical properties of the simulated clouds.

ii. Anthropogenic emission of INPs can exert a strong indirect effect via glaciated clouds.

iii. Time dependence of INP freezing and SIP can significantly affect the radiative properties of the clouds.

3. Aims and Objectives

The research questions addressed in the present study are.

1. To understand the relative importance of a range of biological particles in initiating ice and their effects on the microphysical and macrophysical properties in the simulated continental deep convective clouds.
2. To modify the empirical parametrization in AC to represent the time-dependent approach of INP freezing, using our published laboratory observations of time-dependent INP activity. This objective further investigates the role of the time dependence of the INP freezing process in initiating the observed ice concentrations in a range of cloud systems while accounting for all SIP processes.
3. To investigate the role of various SIP processes in overall ice formation in the simulated continental deep convective clouds. This study also explains the possible cause for the aircraft observed classic dependency of the IE ratio on cloud top temperature in the simulated clouds.
4. To study the mechanisms for the indirect effects from ice nucleus aerosols via glaciated clouds. To investigate the impact from time-dependent INP freezing and SIP on the simulated indirect effects.

These objectives are discussed in four separate papers that are.

3.1 **Paper 1**

The Influence of Multiple Groups of Biological Ice Nucleating Particles on Microphysical Properties of Mixed-phase Clouds Observed during MC3E.

3.2 **Paper 2**

Effects from Time Dependence of Ice Nuclei Activation for Contrasting Cloud Types.

3.3 **Paper 3**

Dependencies of Four Mechanisms of Secondary Ice Production on Cloud-Top temperature in a Continental Convective Storm.

3.4 **Paper 4**

Mechanisms for Indirect Effects from Solid Aerosol Particles on Continental Clouds and Radiation.

4. Description of Numerical Model and Field Campaigns

To address the objectives described in Sec. 2, various observed cloud systems have been simulated with the AC model. These are 1) the Midlatitude Continental Convective Cloud Experiment (MC3E) consisting of deep convective clouds, 2) the Atmospheric Radiation Measurement (ARM) Cloud Aerosol Precipitation Experiment (ACAPEX) characterized by orographic clouds, and 3) the Aerosol Properties, Processes, and Influences on Earth's climate (APPRAISE) consisting of supercooled long-lived stratiform clouds (Sec. 4.2). A brief description of AC is provided below:

4.1 Model Description: Aerosol-Cloud model

The present study used the AC model. AC uses the dynamical core and software infrastructure of the Weather Research and Forecasting (WRF) model (Dudhia 1989; Skamarock et al., 2008) to represent aerosols and clouds with hybrid spectral bin-two-moment bulk microphysics, semiprognostic aerosol, and interactive radiation schemes (Phillips et al., 2007, 2009, 2013, 2015, 2017a, b, 2020). AC uses the WRF schemes of the planetary boundary layer ([PBL], Troen and Mahrt, 1986; Hong and Pan, 1996), subgrid-scale mixing, dynamics, and surface layer. AC has been used in many previous studies (e.g., Kudzotsa et al., 2016a, b, Phillips et al., 2017b, 2018, 2020; Patade et al., 2021; Wa22a; Gupta et al., 2023; Wa23b).

AC represents microphysical species as cloud-liquid and ice ('crystal'), snow, graupel or hail, and rain. The total number and mass ('two-moment approach') mixing ratios of each of these species are diffused and advected as bulk prognostic variables in AC. Mass and number concentrations of ice, initiated through various processes (heterogeneous and homogeneous freezing and SIP) are tagged with prognostic, passive variables in AC. These tagging tracers do not interact with any process in AC. AC initiates cloud droplets by soluble APs, such as ammonium sulfate, sea salt, and soluble organics, at cloud-base (Ming et al., 2006) and at in-cloud levels (Phillips et al., 2007, 2009).

In AC, heterogeneous ice nucleation is governed by a total of eight APs, including mineral dust, soot, insoluble organics, and five PBAPs such as fungi, bacteria, detritus, pollen, and algae (Patade et al., 2021, 2022). AC predicts the INP activity of these APs from the 'empirical parameterization (EP)' (Phillips et al., 2008, 2013). The EP encapsulates all modes of INP activation (Sec. 1.1.2.2) as well as heterogeneous raindrop freezing. The EP depends on the temperature, the surface area mixing ratio of each AP, and supersaturation.

No direct measurements of PBAPs were made during the field campaigns of the simulated clouds. The EP (Phillips et al., 2008, 2013) rather assumed that about 50% of the insoluble organics are biological in origin. The basis for this assumption is previous observational studies of biological particles (Matthias-Maser and Jaenicke 1995; Matthias-Maser et al., 1999, 2000) which reported that biological particles form about 20-30% of the total APs. Furthermore, Jaenicke (2005) observed that about 50% of the total APs are cellular particles. These studies were the basis for Phillips et al. (2008, 2013) to consider about 50% of the insoluble organics as biological in origin. The section below provides a brief description of the original EP representing the time-independent approach of heterogeneous ice nucleation (Phillips et al., 2008, 2013).

4.1.1 Representation of Original EP in AC

In AC, for given aerosol species (X = dust, soot, soluble organics, and PBAPs), the EP gives the number mixing ratio ($n_{IN,X}$) of active INPs (Phillips et al., 2013) at temperature (T),

$$n_{IN,X}(T, S_i, \Omega_X) = \int_{\log[0.1\ \mu m]}^{\infty} \{1 - \exp[-\mu_X(D_X, S_i, T)]\} \times \frac{dn_X}{d\log D_X} \times d\log D_X \tag{1}$$

Where,

$$\mu_X = H_X\,(S_i, T)\xi(T)\left(\frac{\alpha_X n_{IN,1,*}}{\Omega_{X,1,*}}\right) \times \frac{d\Omega_X}{dn_X} \quad \text{for T} < 0°\text{C and } 1 < S_i \le S_i^w \tag{2}$$

Here, Ω_X is the surface area mixing ratio for a given X. The average number of activated ice embryos per insoluble AP of size D_X is given by μ_X. The scarcity of heterogeneous ice nucleation in subsaturated conditions is represented by the empirically determined fraction, H_X which is the function of saturation ratio with respect to ice (S_i) and temperature (T), and it varies between 0 and 1. ξ is the temperature-dependent fraction representing freezing of INP immersed drops and it varies from 0 to 1 for temperatures between -2 and -5°C. S_i^w is the S_i at water saturation. $d\Omega_X/dn_X \approx \pi D_X^2$. The term $n_{IN,1,*}$ is the number of active INPs per kilogram of air and represents the reference activity spectrum of the average concentration of INP. More details are from Phillips et al. (2008, 2013).

Also, insoluble APs may be internally mixed with various soluble APs (Clarke et al., 2004). When the saturation ratio with respect to water (S_w) reaches the critical value, such soluble APs can form cloud droplets, and the insoluble part then becomes immersed in the droplet. The raindrop with immersed INPs in it may nucleate heterogeneously at subzero temperatures to form ice. The equation that gives the number concentration of INPs activated during heterogeneous raindrop freezing ($d(\Delta n_{IN,rain})$) (Phillips et al., 2008) for time-step Δt is,

$$d(\Delta n_{IN,rain}(T, S_i, \Omega_X)) \approx \Delta t\, min\left[(w - v_t)\frac{dT}{dz}, 0\right] \times \frac{d}{dT}\{n_{IN,1,*}[T, S_i^W(T)]\} \sum_X \left(\frac{\alpha_X d\Omega_{X,rain}}{\Omega_{X,1,*}}\right) \quad (3)$$

Here, w is the vertical velocity, v_t is the fall speed of raindrops and $d\Omega_{X,rain} = \Omega_{X,rain}\, dQ_r/Q_r$ denotes the surface area mixing ratio of INP immersed in a raindrop. Also, Q_r is the mass mixing ratio of the raindrop. More details can be found in Phillips et al. (2008).

The number of ice crystals initiated (Δn_i) in a time step (Δt) is incremented by,

$$\Delta n_i = \sum_X \mathrm{MAX}(n_{IN,X} - n_{X,a}, 0) \equiv \sum_X \Delta\, n_{X,a} \quad (4)$$

Here, $n_{X,a}$ is the increment of the number mixing ratio of INPs from group *X* that has been activated.

In summary, Eqs (1)-(4) represent heterogeneous ice nucleation without time dependence.

AC forms ice homogeneously in two ways. The spontaneous freezing of supercooled cloud drops/rain and APs above the -36°C level forms ice. Homogeneous aerosol freezing occurs as soon as the critical supersaturation exceeds. This critical supersaturation depends on the temperature and size of the AP (Phillips et al., 2007).

AC forms secondary ice by four types of ice multiplication mechanisms which are briefly described in Sec 1.1.2. More details of these mechanisms can be found in Phillips et al. (2001, 2003, 2005, 2007, 2017a and b, 2018), Deshmukh et al. (2022), and Wa22.

Furthermore, AC uses our own implementation of the Geophysical Fluid Dynamics Laboratory (GFDL) radiation scheme (Friedreich and Ramaswamy, 1999) in which scattering of SW and LW radiation depends on the effective and generalized effective size of cloud-liquid and cloud-ice. The GFDL radiation scheme used in

AC takes mean sizes of cloud droplets and ice crystals as inputs to calculate the SW and LW fluxes at model levels. This scheme does not predict the direct effect of aerosols.

4.2 Field Campaigns

4.2.1 MC3E

The MC3E campaign was carried out in north-central Oklahoma, collectively by the U.S. Department of Energy (DoE) and ARM climate research facility, and the National Aeronautics and Space Administration's (NASA) Global Precipitation Measurement (GPM). It made observations for a total of 15 data missions focusing on and around the DoE ARM Southern Great Plains (SGP) Central Facility (CF). MC3E took place from 22 April to 6 June 2011 and involved the collection of data from airborne and ground-based measurements (Jensen et al., 2016).

4.2.1.1 Airborne Measurements

During MC3E, the University of North Dakota (UND) Cessna Citation II jet aircraft (Fig. 4a) carrying a standard suite of meteorological instruments together with precipitation, cloud microphysical and liquid and total water content probes (Table 2) made measurements of in-cloud microphysical properties at levels between about 4 and 8 km. The liquid properties (liquid water content [LWC], droplet sizes, and number concentrations) were measured by the cloud droplet probe (CDP) whereas the sizes and number concentrations of ice particles were measured by the 2D cloud (2DC) probe, cloud imaging probe (CIP), and High volume precipitation spectrometer (HVPS-v3). The Combined Spectrum uses particle size distribution of 2DC or CIP merged with HVPS3. The Citation aircraft flew a total of 15 science flights.

Table 2. Details of the optical probes mounted on the sampling aircraft during the field campaigns and corresponding size range considered in the present study.

Campaign	Aircraft	Instruments mounted on the aircraft to measure cloud properties			
		Ice particle	Size range (mm)	Cloud droplet	Size range (µm)
MC3E (11 and 20 May)	UND Citation	2DC CIP HVPS-v3	0.2-1.0 0.2-1.5 0.2-19.2		
ACAPEX	DoE G-1	2DS HVPS	0.2-1.28 0.2-19.2	CDP	2-20
APPRAISE	CFARR UK BAe146	2DS-128	0.1-1.28		

4.2.1.2 Ground-based measurements

The radiosonde array deployed at 6 sites over a 300 km x 300 km area (Jensen et al., 2016) was used to measure the temperature, humidity, and wind properties. Radiosonde observations (Vaisala RS92-SGP) were conducted four times daily to quantify the diurnal cycle of various atmospheric state variables of the environment surrounding the ARM SGP site. The sounding frequency was increased to eight times per day when aircraft operations were occurring based on forecasted convective conditions.

During the MC3E campaign, the spatial variability of moisture, surface heat, and momentum fluxes were measured by the instrumentation included in extended SGP facilities covering an area of about 150 km × 150 km. Measurement of surface precipitation was done with 16 rain gauge pairs placed within a 6 km radius of the SGP CF. Continuous measurements of aerosols, atmospheric gases, meteorological conditions (e.g., temperature, precipitation, wind), and clouds were conducted by the dedicated instrumentation suite deployed at the ARM SGP CF.

The CCN number concentrations were measured by a CCN counter (DMT) at seven levels of supersaturation (Jefferson, 2011; Uin, 2022) at Lamont, Oklahoma whereas no measurements of INPs were made during the MC3E campaign. Large-scale forcing (LSF), surface heat, and moisture fluxes were derived from a constrained variational analysis approach (Jensen et al., 2016).

The case considered here is a line of convective clouds observed during MC3E on 11 May 2011. These clouds had warm bases near 17°C at about 1.5 km altitude above mean sea level (MSL). The ground level was about 350 m MSL. The convective line, a type of an MCS consisted of different cloud types, most of which were deep convective (e.g., cumulonimbus) with typical cloud depths of 9-13 km and stratiform clouds. Figure 4a shows the study domain. Figure 4b shows the profiles of air and dewpoint temperature on 11 May at 12:00 UTC derived from AC. The lifting condensation level (LCL) was at about 870 hPa (17°C) and the predicted convective available potential energy (CAPE) was about 2200 J kg^{-1} (Fig. 4b), which is mostly attributed to the moistening of the lower troposphere from large-scale advection (Jensen et al., 2016). The horizontal wind speed is relatively high (> 15 m s^{-1}) throughout the atmosphere.

Figure 4(c-e) shows images of ice particle habits from the CIP, mounted on the Citation aircraft (Fig. 4a), at various levels in convective cloudy updrafts ($w > 1$ m s^{-1}). These profiles show that the levels near the cloud base are mostly dominated by raindrops (0.2 to 1 mm, Fig. 4c). Furthermore, the higher levels (-7 to -18°C) are observed to be dominated by aggregates and rimed ice particles (Fig. 4d-e) whereas, pristine ice crystals are relatively less at these levels.

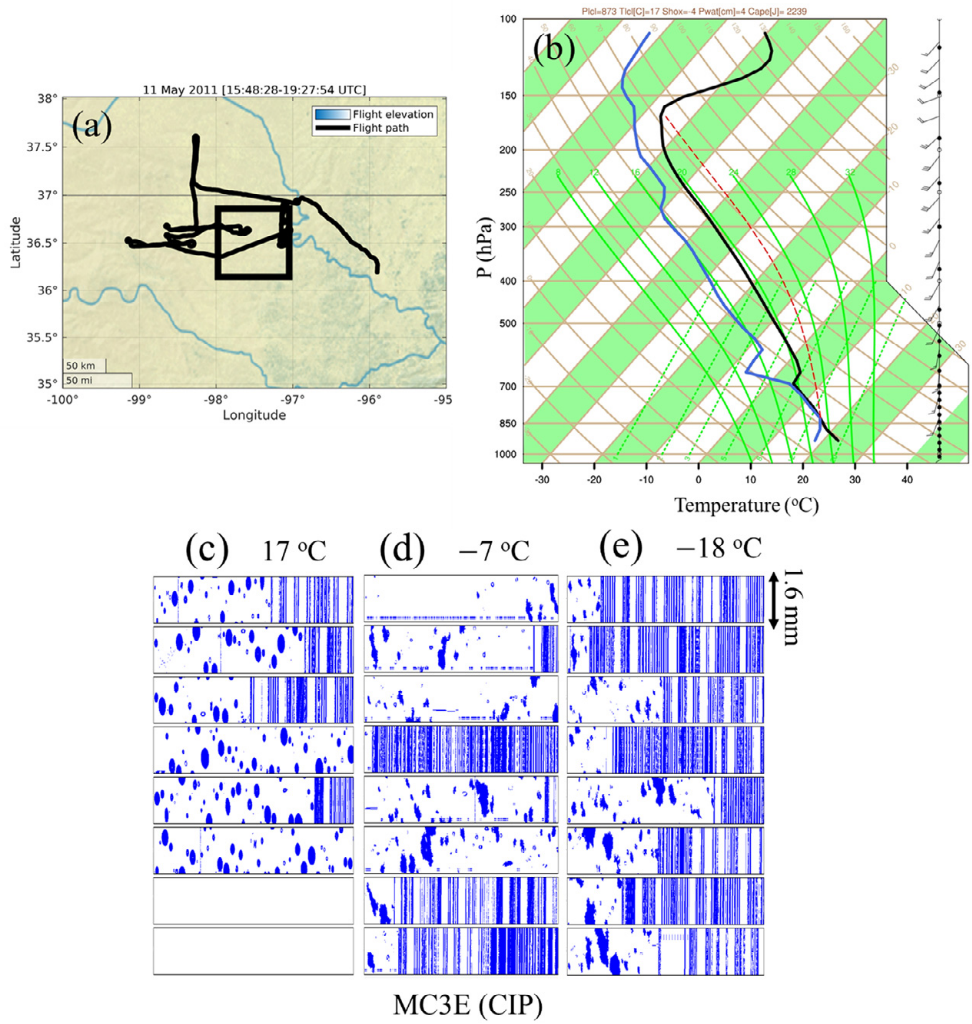

Figure 4. (a) Profiles of geographical area, flight track of the UND Citation aircraft (thin black line) and the simulation domain (solid black box), (b) the vertical profile of the air (solid blue line) and dewpoint (solid black line) temperature, and moist adiabat (dotted red line) on 11 May 2011 at 12:00 UTC. Also shown are the ice particle habits in convective cloudy updrafts ($w > 1$ m s^{-1}) at (c) 17°C, (d) −7°C, (d) −18°C from the CIP mounted on the UND Citation aircraft during the MC3E campaign on the same day.

Also, another case of a squall line was observed on 20 May 2011 (00:00-24:00 UTC), in which convection was triggered by a flow of moisture from the Gulf of Mexico (Jensen et al., 2016; Patade et al., 2022). The main convective event was observed between 10:30 and 11:00 UTC, with a peak precipitation rate of about 6 mm hr^{-1}, followed by widespread stratiform precipitation. The instruments described above were used to measure the properties of these clouds. The bases of the clouds were at about 20°C whereas their tops were extending up to the tropopause level (about −60ºC). More details about soundings, LSF, and other meteorological conditions are from Patade et al. (2022).

4.2.2 ACAPEX

ACAPEX was a multiagency field campaign designed to understand the effects on the amount and phase of precipitation associated with atmospheric rivers (AR) from aerosols from local pollution and from long-range transport (Leung 2016). ACAPEX was carried out between 12 January and 8 March 2015 as a part of CalWater-2015. The CalWater-2015 project included four aircraft: 1) DoE Gulfstream-1 (G-1), 2) NASA ER-2, and the National Oceanic and Atmospheric Administration (NOAA) 3) G-IV, and 4) P-3 aircraft. The DoE G-1 aircraft sampled clouds between the Central Valley and Sierra Nevada jointly with the NOAA *Ron Brown* ship. The Ron Brown ship made measurements of temperature, humidity, winds, and radiative and surface fluxes and was carrying the ARM Mobile Facility 2 (AMF2) which made the measurements of aerosols and clouds.

The CDP and 2D spectrometer (2DS) and HVPS probes (Table 2) mounted on the DoE G-1 (Fig. 5a) aircraft respectively measured the liquid and ice properties of the ACAPEX clouds. Furthermore, the surface precipitation was measured with rain gauges deployed on the ground at several locations. The case analyzed here involved orographic clouds with embedded convection that brought significant precipitation over the US west coast (Northern California) due to the landfall of an AR on 7 February 2015 (19:00-23:00 UTC).

Figure 5(b-d) shows images of hydrometeor habits observed in the ACAPEX campaign from the 2DS probe at various levels in the cloudy convective updrafts (w > 1 m s^{-1}). From these profiles, it is evident that the levels near the cloud base were dominated by raindrops (0.2 to 1 mm, Fig. 5c). Furthermore, mostly pristine ice particles were observed at subzero levels warmer than −7ºC whereas, levels above −7ºC were mostly dominated by aggregates and rimed ice particles.

The Hybrid Single-Particle Lagrangian Integrated Trajectory (HYSPLIT) backward trajectory plotted for 120 hrs shows that over the study domain, APs are mainly marine in origin (Fig. 5e) whereas, dust and black carbon were less (Levin et al., 2019; Lin et al., 2022). The profiles of the air and dewpoint temperatures from AC are shown in Fig. 5e. From this profile, it can be seen that the LCL is at about 10ºC (930 hPa), and the wind speeds were observed to be relatively high (about 10 m s^{-1}) throughout the atmosphere whereas, the CAPE is relatively low (500 J kg^{-1}).

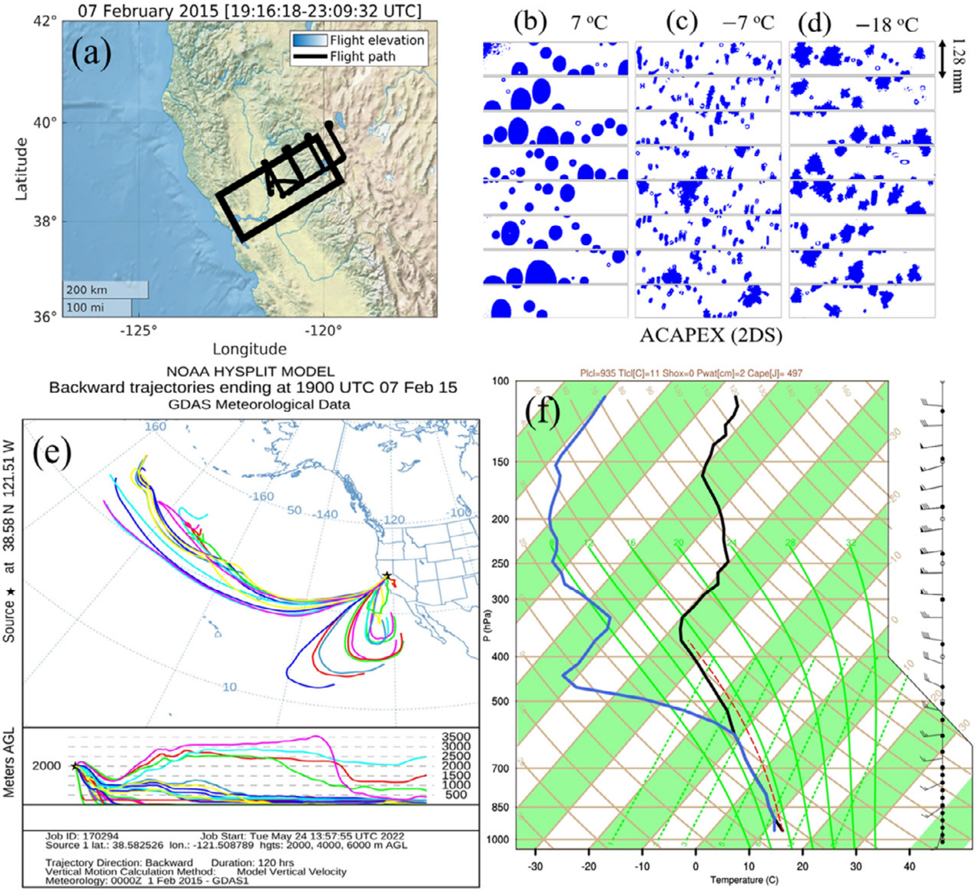

Figure 5. (a) Profiles of geographical area, flight track of the DoE G-1 aircraft (thin black line) and the simulation domain (solid black box), and the ice particle habits in convective cloudy updrafts (w > 1 m s^{-1}) at (c) 7ºC, (d) –7ºC, (d) –18ºC from the 2DS probe mounted on the DoE G-1 aircraft during the ACAPEX campaign on 07 February 2015. Also shown are the (e) HYSPLIT backward trajectory for 120 hrs showing the airflow from the North Pacific Ocean over the study domain (Sacramento, California, USA) and (f) the vertical profile of the air (solid blue line) and dewpoint (solid black line) temperature and moist adiabat (dotted red line) on the same day at 19:15 UTC.

4.2.3 APPRAISE

APPRAISE was carried out in the winter 2009 over the southern UK to study the microphysical processes associated with liquid and ice-phase formation in mixed-phase frontal clouds. A case analyzed here was anticyclonic (surface pressure 1020 hPa) consisting of the episodes of: 1) weak embedded convection (00:00-12:00 UTC), and 2) layer clouds (12:00-24:00 UTC) on 18 February 2009 during the APPRAISE campaign (C11; WI13; Wa23a) and covering an area of more than 100 km in width (C11; WI13). The observed cloud base was at about 6ºC whereas the cloud top was quasi-steady throughout the day (cooling by about 1.5 K), extending up to −15ºC (Fig. 6f). Both the episodes of the APPRAISE clouds were observed to precipitate throughout the day (C11; WI13).

The 2DS and CDP probes (Table 2) mounted on the Chilbolton Facility for Atmospheric and Radio Research (CFARR) BAe-146 aircraft (Fig. 6a) carried out the measurements of ice and liquid properties of the APPRAISE clouds near the CFARR. To validate the AC predicted ice concentrations (> 0.1 mm), corrections are applied to the observations from the 2DS probe by multiplying all measured ice concentrations (WI13, their Fig. 9) by a factor of 0.253 following Korolev et al. (2011, their Fig. 5).

Figure 6(b-e) shows particle habits observed from the 2DS probe on 18 February 2009 between levels −4.3 and −11.7ºC in convective cloudy regions (adopted from C11). These images show the majority of rimed ice particles at about −7ºC level whereas the levels near cloud top (−12ºC, Fig. 6e) were dominated mostly by pristine ice crystals such as plates and aggregates. The lower levels (−4.3ºC, Fig. 6b) were dominated by small columns. This was the basis for C11 to propose the activity of SIP through the HM process in the episode of weak convection of the APPRAISE clouds.

Figure 6f illustrates the profiles of the air and dew-point temperatures on 18 February 2009 at 00:00 UTC derived from AC. The predicted horizontal wind speeds are significantly weak (< 3 m s^{-1}) and are south-westerly in the lower troposphere. Levels above the cloud top show a temperature inversion (temperature difference of about 4ºC) layer characterized by extremely low relative humidity (RH < 50%). For APPRAISE, as reported by WI13 and Wa23a, for the layer cloud episode, two distinct cloudy layers are seen: 1) a saturated layer at levels between about cloud-base and 1.2 km, and 2) a thin, supersaturated layer at levels above 2.5 km extending up to 4 km. These two layers are separated by a subsaturation layer (about 1 km thick). The majority of APs were marine in origin with a mixture of continental aerosols from various parts of Western Europe. C11, WI13, and Wa23a provide more details of the observed system.

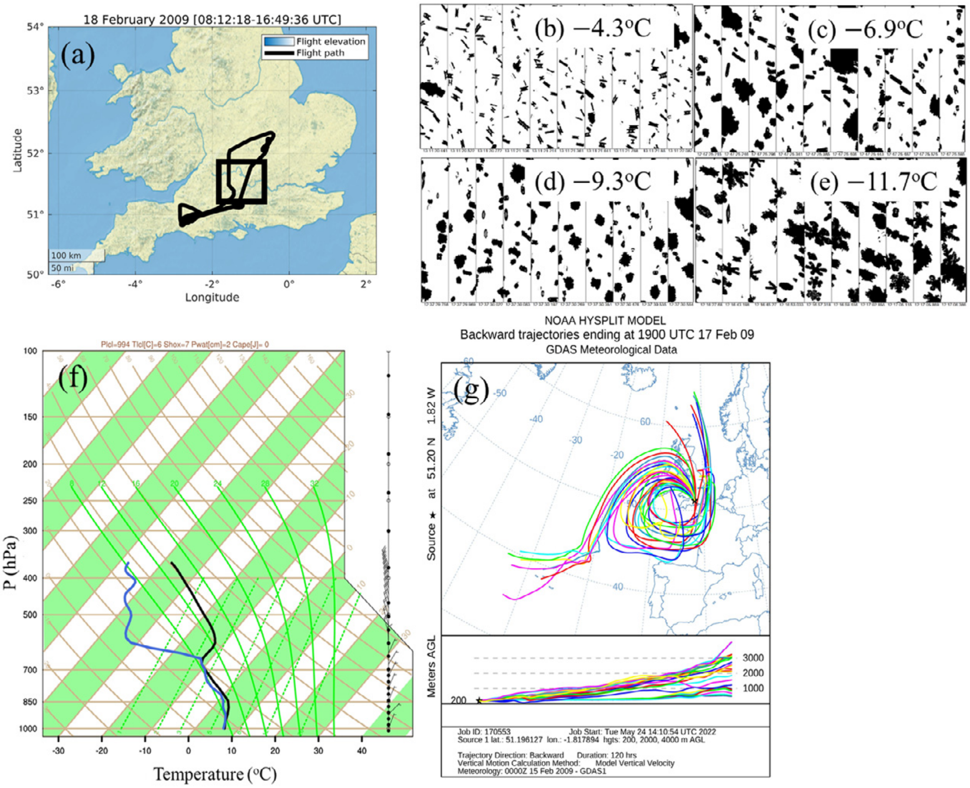

Figure 6. (a) Profiles of geographical area, flight track of the BAe146 aircraft (thick black line) and the simulation domain (solid black box) during the APPRAISE campaign on 18 February 2009, and particle images at (b) −4.3ºC, (c) −6.9ºC, (d) −9.3ºC and, (e) −11.7ºC from the 2DS probe mounted on the BAe146 aircraft (adopted from C11), Each image strip is approximately 12.8 mm long and 1.28 mm wide. Also shown are the (f) vertical profile of the air (solid blue line) and dewpoint (solid black line) temperature at 00:00 UTC for the same day and, (g) HYSPLIT backward trajectory for 120 hrs showing the airflow from the North Atlantic Ocean region as well as from polluted regions such as France over the study domain (Larkhill, UK).

5. Methodology

Four cloud cases (Sec. 4.2) were simulated with AC for a 3D mesoscale domain (Sec. 4.1) to address the research questions outlined in Sec. 2. All these cloud cases are simulated in an idealized manner, wherein no attempt was made to estimate the precise cloud locations. The horizontal (along x and y directions) and vertical resolution of the simulation domain are about 2 and 0.5 km respectively, and the model integration time step is about 10 sec. For the simulated APPRAISE and MC3E (both 11 and 20 May 2011) clouds, the lateral boundary conditions are periodic in both x and y directions. On the other hand, for the ACAPEX case, boundary conditions are open and periodic in x and y directions, respectively. The model top was at about 16 km for the MC3E and ACAPEX simulations, and about 8 km for the APPRAISE case.

Regarding the simulation period, during MC3E, an MCS observed on 11 May 2011 is simulated for 72 hours from 10 May 00:00 to 13 May 00:00 UTC whereas a squall line observed on 20 May 2011 is simulated for 48 hours between 20 May 00:00 and 21 May 00:00 UTC. Also, a case of supercooled layer clouds observed during APPRAISE is simulated for 48 hours from 17 February (00:00 UTC) to 19 February 2009 (00:00 UTC). Furthermore, a case of orographic clouds in ACAPEX observed on 7 February 2015, is simulated for 3 hours from 19:15 to 22:15 UTC.

More details about the domain set-up for these simulated cases are from Patade et al. (2022), Wa22, and from Wa23a.

A brief description of the model set-up, modifications made in the scheme of the heterogeneous ice nucleation process, and the sensitivity tests carried out for each paper (Sec. 3) is provided below:

5.1 Paper 1

The Influence of Multiple Groups of Biological Ice Nucleating Particles on Microphysical Properties of Mixed-phase Clouds Observed during MC3E.

To study the influence from various groups of PBAPs on the micro- and macrophysical properties of the convective storm, a case of deep convective clouds observed during the MC3E campaign on 20 May 2011 (Sec. 4.2.1) was simulated with AC.

The EP proposed by Phillips et al. (2008, 2013) initiates ice via the activity of APs such as mineral dust, soot, soluble organics, and PBAPs. However, this EP did not resolve the individual groups of PBAPs. Based on the field observations from Amazonia, Patade et al. (2021) proposed an empirical formulation to predict the INP activity of five types of PBAPs including 1) fungi, 2) bacteria, 3) pollen, 4) algae, and 5) plant/animal detritus. This empirical formulation is an extension of the original EP (Phillips et al., 2008, 2013) (Sec. 4.1.1), and is based on the observed properties of PBAPs such as their sizes, biological composition, number concentrations, and ice nucleating ability. Furthermore, it is dependent on parameters such as T, S_i, and the surface area mixing ratio of a given aerosol species. More details are from Patade et al. (2021, 2022).

5.2 Paper 2

Effects from Time Dependence of Ice Nuclei Activation for Contrasting Cloud Types.

To estimate the effects from time-dependent INP freezing on overall ice concentration in clouds, three cloud cases (Sec. 4.2) have been simulated with AC (Sec. 4.1). These include 1) supercooled layer clouds observed during APRPAISE on 17 February 2009, 2) orographic clouds with embedded convection observed on 7 February 2015 during ACAPEX, and 3) deep convective clouds observed during MC3E on 11 May 2011.

To evaluate the role of time-dependent freezing of various INP species (Sec. 4.1), the original EP (Sec. 4.1.1; Phillips et al., 2013; Patade et al., 2021) was modified by a purely empirical approach in light of the laboratory observations of time dependence by JK22. The modifications made in the original EP (Sec. 4.1.1) to represent the time-dependent approach of INP freezing are described below.

5.2.1 Modification to original EP in AC to Represent Time Dependence of INPs

An experimental study by JK22 quantified the time dependence of INP activity in freezing mode. They considered various aerosol classes such as rural continental, continental polluted, continental pristine, combustion dominated, mineral dust influenced and marine dominated. JK22 observed an increment in INP concentrations by 70 to 100% (70 to 200%) over the period of 2 to 10 hours and the maximum time dependence for dust and rural continental samples.

JK22 proposed the temperature-shift ($\Delta T_X = \Delta T_X(t^*) \leq 0$) approach to represent the time-dependent freezing of active INPs. The original EP (Sec. 4.1.1), representing heterogeneous ice nucleation, was modified by adding the temperature shift for each AP to represent a time-dependent approach of INP freezing, following JK22 (their Sec. 3.2.2).

The temperature-shift is (JK22),

$$\Delta T_X(t^*) = -A_X {t^*}^{\beta} \tag{5}$$

Here, t^* is the time since the parcel entered the glaciating part of a cloud (the age of the cold parcel). Here, t^* is estimated by a passive tracer (Q) that decays exponentially with time following the motion of any parcel in a cold cloud (T < 0°C and ice water content [IWC] > 10^{-6} kg m^{-3}). The evolution of Q is from numerical integration during the simulation of:

$$\frac{dQ}{dt} = \begin{cases} \frac{-Q}{\tau_Q} & \forall\, T < 0\text{°C and } IWC > 10^{-6}\ \text{kg m}^{-3} \\ 0 & \text{otherwise} \end{cases} \tag{6}$$

Here, τ_Q is an arbitrary relaxation time and is set to 1800 seconds throughout the simulation. For an adiabatic parcel, the analytical solution of Eq (6) gives t^*,

$$t^* \approx -\tau_Q \ln(Q/Q_0) \tag{7}$$

Outside of the cold cloud, $Q = Q_0 = 1\ \text{kg}^{-1}$ is prescribed everywhere. Effects on t^* from dilution of actual simulated parcels are approximately represented by virtue of in-cloud mixing and entrainment being treated in the numerical prediction of Q.

With this temperature-shift ($\Delta T_X(t^*)$), the time-dependent number mixing ratio of active INPs ($\tilde{n}_{IN,X}$) in the X-th species from Eq (1) is,

$$\tilde{n}_{IN,X}(T, S_i, \Omega_X, t) = n_{IN,X}\left(\left(T + \Delta T_X(t^*)\right), S_i(T + \Delta T_X(t^*)), \Omega_X\right) \tag{8}$$

Similarly, the time-dependent number mixing ratio of INPs activated in heterogeneous raindrop freezing ($d(\Delta\tilde{n}_{IN,rain})$) from Eq (4) is obtained by summing over each raindrop size bin,

$$d\left(\Delta\tilde{n}_{IN,rain}(T, S_i, \Omega_X)\right) = d\left(\Delta n_{IN,rain}(T + \Delta T_X(t^*), S_i(T + \Delta T_X(t^*)), \Omega_X)\right) \tag{9}$$

More details can be found in JK22 and in Wa23a.

Two simulations were performed to evaluate the role of the time dependence of INP freezing in forming overall ice in the simulated clouds. These are, 1) the control run which includes time-dependent INP freezing, all SIP mechanisms, and homogeneous ice nucleation, and 2) the 'no time-dependent INP' run in which time dependence of INP freezing is excluded from the control run. Additionally, one more sensitivity test ('no dust from droplet evaporation') was carried out in order to analyze the mechanisms responsible for the continuous nucleation of ice in the episodes of the simulated APPRAISE clouds (Wa23a). In this test, the contribution to dust particles in the air is excluded from droplet evaporation from the control run. More details are from Wa23a.

5.3 Paper 3

Dependencies of Four Mechanisms of Secondary Ice Production on Cloud-Top temperature in a Continental Convective Storm.

Aircraft observations of young, ascending cumulus clouds over Miles City, Montana, USA by Hobbs et al. (1980, their Fig. 25) showed the classic dependency of IE ratio on cloud-top temperature. They observed a classic peak in IE ratio at a characteristic cloud-top temperature of about -12^{o}C. However, the SIP mechanisms responsible for this classic dependency were unknown at that time. In this paper, an attempt was made to analyze the causes for this classic dependency by simulating a similar event of convective clouds observed during MC3E on 11 May 2011 (Sec. 4.2.1), partly using tagging tracers (Sec. 4.1).

Here, the IE ratio is defined as the ratio of the number concentrations of the average non-homogeneous ice (total homogeneous ice minus total ice from cloud ice and snow) at any in-cloud level to that of INPs active at cloud-top. In this study, young, developing cumulus clouds were sampled using the cloud-top algorithm (Wa22, their appendix A). The predicted age of these clouds is between 5 and 30 min. More details are from Wa22.

5.4 Paper 4

Paper 4 involved the study of the net AIEs from ice-nucleating aerosols. Also, the impact from the time dependence of INP freezing and SIP on the predicted net AIEs is investigated. This is achieved by performing a series of sensitivity tests with AC for the simulated APPRAISE and MC3E (11 May) clouds. This involved modifications in the control run to create various perturbation simulations. The control run (Table 3) here is referred to the simulation that includes time-dependence of heterogeneous ice nucleation (Sec. 5.2.1), homogeneous freezing, and all four SIP processes (Sec. 1.1.2). This control run is simulated for the present-day as well as pre-industrial solid aerosol conditions. Furthermore, both present-day and pre-industrial simulations have been performed with the present-day thermodynamic conditions to eliminate any radiative forcing arising from changing thermodynamic forcing.

In the pre-industrial simulation, solid aerosols are prescribed with an adjustment factor derived from a modelling study of the global distribution of APs from the pre-industrial (1850) to future projection (2100) by Takemura (2012). They reported that the present-day soot concentration is a factor of about 2.5 higher compared to 1800 and is the most affected AP among all solid APs due to anthropogenic activities. Furthermore, in present-day conditions, Takemura (2012) reported a factor of about 1 increase in mineral dust particle concentrations relative to 1800 whereas, no significant change is seen in soluble organics and biological particles.

To estimate the albedo-emissivity and lifetime indirect effects of solid aerosols in the simulated supercooled, mixed-phase layer clouds (APPRAISE) and convective storm (MC3E), various sensitivity tests have been performed following the techniques used in Kudzotsa et al. (2016b). These sensitivity tests are classified as Tests A and B predict the net albedo-emissivity and lifetime indirect effect, respectively for a targeted cloud type. Kudzotsa et al. (2016b) and Wa23b gives more details about these sensitivity tests. However, they are briefly described below.

Table 3. Description of the simulations performed for the simulated APPRAISE and MC3E cases. Each simulation is performed with the present-day and pre-industrial aerosol conditions.

Simulation	Description
Control	Includes time dependent INP freezing, all SIP and homogeneous freezing
No SIP	Excludes all SIP processes from the control run
No time dependent INP	Excludes time dependent INP freezing from the control run

5.4.1 Net Indirect Effects from Anthropogenic Solid Aerosols

A. Test A: The Total and Albedo-Emissivity AIE

The total or net (Q_{net}) AIE is the difference in net radiative fluxes at the TOA (at the model top) between the present-day ($Q_{PRESDAY}$) and pre-industrial (Q_{PREIND}) run, simulated in the control environment (Gettleman et al., 2012; Lohmann, 2006; Kudzotsa et al., 2016b).

$$Q_{net} = Q_{PRESDAY} - Q_{PREIND} \quad (10)$$

The albedo of a given cloud is strongly dependent on the mean sizes of cloud hydrometeors (cloud-liquid and ice-crystal), and changing aerosol conditions due to anthropogenic activity can significantly alter the mean sizes of these cloud particles, giving rise to albedo-emissivity AIE. To evaluate the albedo-emissivity AIE of a targeted cloud type, two model runs are performed with two calls to the radiation scheme. The first call is an active call, in which properties of hydrometeors, such as sizes and number concentrations, are dependent on aerosol loading. By contrast, the second call is a passive call, which means hydrometeor properties are independent of changes in aerosol loading. This passive call does not alter the microphysics of the simulation. This is achieved by creating temperature and vertical-velocity-dependent look-up tables of mean sizes and/or number concentrations of cloud droplets and ice crystals. These look-up tables are designed from the control simulation. The same look-up tables have been used for both the control and pre-industrial simulations.

The difference in the net radiative fluxes at the TOA between the control and pre-industrial runs predicted from the first calls gives the Q_{net}. Furthermore, if the same approach is applied to the second calls of both the control and pre-industrial simulations, a hypothetical net radiative flux (Q_{net_life}) can be estimated, which is the total lifetime AIE. Finally, the albedo-emissivity AIE is given by subtracting Q_{net_life} from Q_{net}.

$$Q_{net\_alb} = Q_{net} - Q_{net\_life} \tag{11}$$

If the approach discussed above is applied to a targeted cloud type, then the corresponding albedo-emissivity AIE can be estimated. For example, to estimate the albedo-emissivity indirect effect of glaciated clouds, the cloud-droplet and ice crystal mean sizes are defined using look-up tables in glaciated clouds. Similarly, the albedo-emissivity AIE of ice-only clouds is predicted by prescribing the mean sizes of these hydrometeors in ice-only clouds. At a given time step in the simulation, a grid point is said to be *ice-only* when it has zero cloud-liquid and non-zero cloud-ice mass mixing ratios. On the other hand, above the freezing level (0ºC), model grid points containing non-zero cloud-liquid and/or cloud-ice mass mixing ratios are identified as *glaciated* clouds.

B. Test B: The lifetime AIE

i. Lifetime AIE for Glaciated Clouds

The lifetime indirect effect for a targeted cloud type is estimated by eliminating the responses of the corresponding microphysical processes using the look-up tables of the mean sizes and/or number concentrations of cloud hydrometeors. For example, to estimate the lifetime effect of glaciated clouds, indirect effects from liquid-only clouds are prohibited by using the look-up tables of the mean sizes and number concentrations of cloud-liquid in the microphysical processes such as collision and coalescence, auto-conversion, sedimentation as well as radiative properties.

The difference in the TOA net radiative fluxes between the present-day and pre-industrial runs performed with look-up tables for these microphysical processes and with passive second calls to the radiation scheme gives the net radiative flux without any indirect effects from water-only clouds at levels warmer than 0ºC (Q_{hyp_glc}). Finally, subtracting the Q_{alb_glc} (test A) from Q_{hyp_glc} gives the estimate of the lifetime indirect effects from glaciated clouds (Q_{life_glc}).

ii. Lifetime AIE for Ice-only and Mixed-phase Clouds

To estimate the lifetime indirect effects from ice-only clouds, the responses of the aerosol-dependent microphysical processes of ice-only clouds are eliminated from the present-day and pre-industrial simulations by using the look-up tables of ice crystal number concentrations and sizes. Yet, responses of microphysical processes to changes in aerosol loading are allowed in mixed-phase and liquid-only clouds. The microphysical processes associated with ice-only clouds are auto-conversion of cloud-ice to snow, sedimentation of cloud-ice, aggregation of graupel and cloud-ice, and aggregation of cloud-ice with snow. Additionally, the passive second call to the radiation scheme is used with the same look-up table for ice-only clouds to eliminate their albedo-emissivity effect.

The difference in the TOA net radiative fluxes between the present-day and pre-industrial simulations, performed using the look-up tables for these microphysical processes and radiative properties in ice-only clouds, gives a hypothetical net radiative flux for liquid-only and mixed-phase clouds ($Q_{hyp\_net\_liq\_mix}$). Subtracting $Q_{hyp\_net\_liq\_mix}$ from the Q_{net} determined in Test A gives the net indirect effects from ice-only clouds (Q_{net_ice}). Finally, subtracting Q_{alb_ice} from Q_{net_ice} gives the lifetime indirect effects from ice-only clouds (Q_{life_ice}).

Furthermore, the indirect effects from mixed-phase clouds are determined by subtracting the indirect effects of ice-only clouds from those of glaciated clouds.

5.4.2 SIP and Time dependent INP freezing Indirect Effects

To estimate the effects on the net AIEs predicted above (Sec. 5.4.1, Tests A and B), arising from SIP and time-dependent INP freezing, two perturbation simulations are performed by altering the control simulations (Table 3). These are 1) a 'no SIP' run in which SIP is completely prohibited from the control simulation, and 2) a 'no time-dependent INP' run in which time dependence of INP freezing is prohibited from the control run. These simulations are carried out for the present-day as well as pre-industrial solid aerosol conditions. In these simulations, the indirect effects for each cloud type are estimated by repeating Tests A and B described above (Sec. 5.4.1). Note that separate lookup tables for particle mean sizes and number concentration are used to perform 'no SIP' simulations. These lookup tables are temperature and vertical velocity dependent and are designed from the present-day 'no SIP' simulation. However, the same look-up tables for particle mean sizes and number concentrations from the present-day control run are used to perform 'no time-dependent INP' simulations. Finally, by subtracting the AIEs from 'no SIP' and 'no time-dependent INP' runs from the net AIEs predicted in the control run, gives the 'SIP' and 'time-dependent INP' indirect effects.

6. Results and Discussion

The study presented here addresses a broad range of research questions in the field of ice microphysics such as, 1) the role of different groups of biological particles in initiating overall ice concentration, and altering the micro- and macrophysics of the clouds (Paper I), 2) the importance of time dependence of INP freezing in initiating overall ice concentration in various cloud systems and its role in precipitation formation (Paper II), 3) dependency of various SIP mechanisms on cloud-top temperature and their evolution in a convective storm (Paper III), and 4) indirect effects from anthropogenically increased solid aerosols and impacts on these AIEs from ice formation processes in the simulated deep convective and supercooled layer clouds (Paper IV).

Such a broad analysis of various ice formation processes and radiative responses of clouds is only made possible with AC which is a state-of-the-art numerical model (Sec. 4.1). AC is designed in the WRF model framework and predicts both number and mass mixing ratios (double-moment approach) of cloud microphysical species such as cloud-liquid, cloud-ice, rain, snow, graupel/hail. Furthermore, AC has a semi-prognostic aerosol scheme and uses the GFDL radiation scheme interactively with cloud properties. AC provides a special advantage to track the number and mass mixing ratios of cloud-ice and snow initiated from various processes (heterogeneous and homogeneous nucleation and all four mechanisms of SIP) by prognostic variables known as tagging tracers (Sec. 4.1).

To address the research questions and to test the hypotheses described in Sec. 2, four cloud systems have been simulated using AC for a 3D mesoscale domain. These include events of summertime deep convection observed over Oklahoma, USA during the MC3E campaign on 1) 11 May 2011 and on 2) 20 May 2011, and wintertime 3) orographic clouds with embedded convection observed during the ACAPEX campaign over California on 7 February 2015, and 4) supercooled stratiform clouds observed on 17 February 2009 over Larkhill, UK during the APPRAISE campaign.

A striking feature of AC is that it adequately predicts the observed filtered ice particle number concentrations at all sampled levels in all four simulated cases. The reason for this adequate validation of ice particle number concentrations is mainly the general realism of the representation of all four SIP mechanisms in AC. Furthermore, other cloud properties such as LWC, cloud droplet mean sizes and number concentrations, surface precipitation, TOA radiative fluxes, and radar reflectivity have also been validated adequately with the coincident observations from aircraft, ground-based instruments and from satellite for the simulated cases. It is further predicted that all these validated microphysical and macrophysical properties differ by less than ±30% from the coincident observations in all the simulated cloud systems.

A brief summary of results and discussions from each paper are given below:

6.1 Paper 1

The Influence of Multiple Groups of Biological Ice Nucleating Particles on Microphysical Properties of Mixed-phase Clouds Observed during MC3E

In this objective, the role of various groups of PBAPs as INPs is investigated in a simulated squall line observed on 20 May 2011 during MC3E. This is done by modifying the original EP (Phillips et al., 2013) in light of the formulation proposed by Patade et al. (2021), which is based on the field observations of various groups of PBAPs from Amazonia. The groups of biological particles analyzed here include fungal spores, pollen, bacteria, animal and plant detritus, and algae.

In the simulated MC3E clouds, it is predicted that the ice nucleus activity of all PBAPs forms only about 1% of the overall active INPs (Fig. 7a, b). The overall weakness of the simulated activity of PBAP INPs can be attributed to their low concentrations compared to other INPs over the study domain.

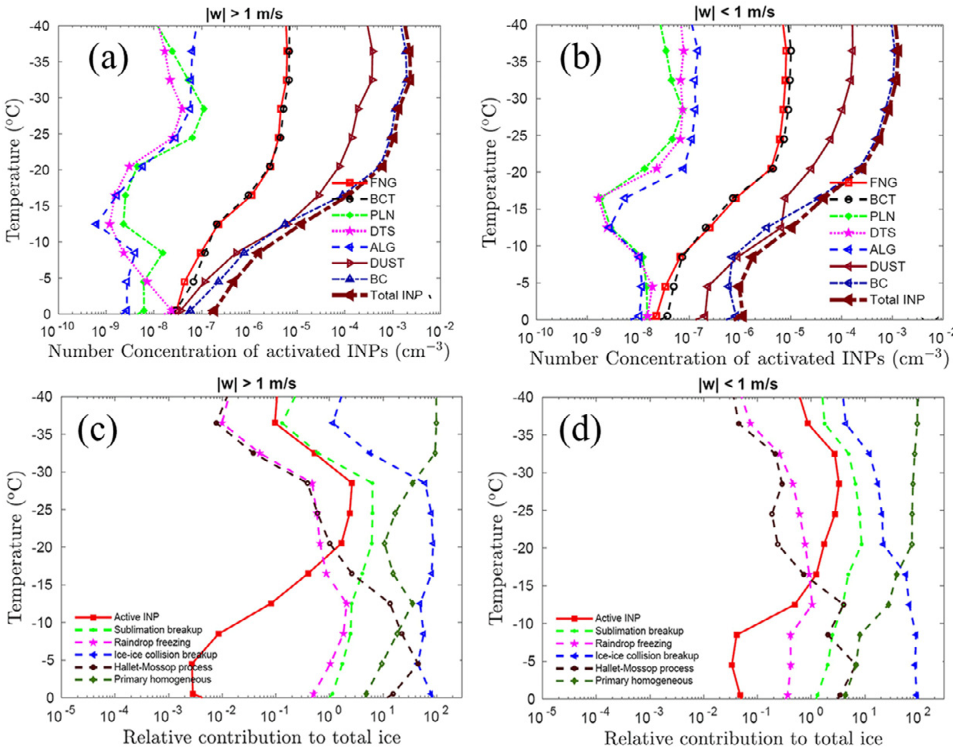

Figure 7. Predicted number concentrations of activated INPs from various PBAP species such as fungi (squares), bacteria (circles), pollen (asterisks), detritus (stars), and algae (backward pointing triangles) along with dust (forward pointing triangles) and black carbon (upward pointing triangles) as well as the total INPs, conditionally averaged for (a) convective ($|w| > 1$ m s^{-1}), and (b) stratiform ($|w| < 1$ m s^{-1}) regions in the simulated squall line observed during the MC3E (20 May 2011) campaign. Also shown is the relative contributions to the total ice concentrations from active INPs (squares), ice from homogeneous (pluses) and from various SIP processes such the HM process (circles), and from fragmentation during ice-ice collisions (backward pointing triangles), raindrop freezing (stars), and sublimation of dendritic snow and graupel (green line). All these quantities (a-d) from advective tagging tracers for the given process and are conditionally averaged for the (c) convective ($|w| > 1$ m s^{-1}), and (d) stratiform ($|w| < 1$ m s^{-1}) regions (adopted from Patade et al., 2022).

The conclusions from the validated simulation of a squall line from MC3E are as follows:

i. Regarding INP activity, at subzero levels warmer than −12°C, the overall INP concentration is chiefly (about 70-80%) from soot and mineral dust INPs. On the other hand, at levels colder than −12°C, soot INPs initiate about 95% of the total INP concentrations (Fig. 7a, b).

ii. At subzero levels warmer than −36°C, primary ice and SIP (through the HM process and fragmentation in ice-ice collisions) are predicted to initiate about 1% and 99% of the overall ice concentration respectively (Fig. 7c, d).

iii. Each PBAP group has different ice nucleation properties in terms of their efficiency of nucleating ice and onset temperatures.

iv. Processes of ice initiation such as heterogeneous and homogeneous ice nucleation and SIP have the least sensitivity with respect to PBAP INPs (Fig. 7c, d).

In summary, it is predicted that the groups of PBAPs predict the modest ice nucleus activity in the simulated convective storm. It is instead predicted that, in such continental convective clouds, the active INP number concentrations of mineral dust and soot are higher by about 1 (at −15°C) and 2 (−30°C) orders of magnitude than PBAP INPs. A more detailed discussion is from Patade et al. (2022). To conclude, PBAPs cause no significant change in the predicted microphysical and macrophysical properties of the simulated MC3E clouds.

6.2 Paper 2

Effects from Time Dependence of Ice Nuclei Activation for Contrasting Cloud Types

This paper investigates the role of time-dependent heterogeneous ice nucleation in overall ice initiation in the simulated summertime deep convection (MC3E, 11 May 2011), and wintertime orographic clouds with weak embedded convection (ACAPEX) and supercooled stratiform (APPRAISE) clouds. This is achieved by modifying the original EP in AC (Phillips et al. 2013) in light of the formulation proposed for time-dependent INP freezing by JK22, as discussed in Sec. 5.2. Furthermore, properties such as the mean sizes and number concentrations of cloud droplets, their LWC, and number concentrations of ice particles larger than 200 μm (in ACAPEX and MC3E), and 100 μm (in APPRAISE) predicted from the control simulations of the simulated cloud cases have been validated adequately with the coincident aircraft and ground-based measurements.

For all the simulated cases (MC3E, ACAPEX, and APPRAISE), it is predicted that the overall ice concentration is mostly dominated by various SIP mechanisms (Fig. 8b, d, f). By contrast, the inclusion of time-dependent INP freezing in the control runs of the simulated cases initiates about half an order of magnitude (in APPRAISE), and about 10% (in ACAPEX and MC3E) more ice particles. This is mostly due to the activity of dust and soot APs (10-50% increase, Fig, 8a, c, e), which is consistent with the previous laboratory observations (Wright et al., 2013; JK22).

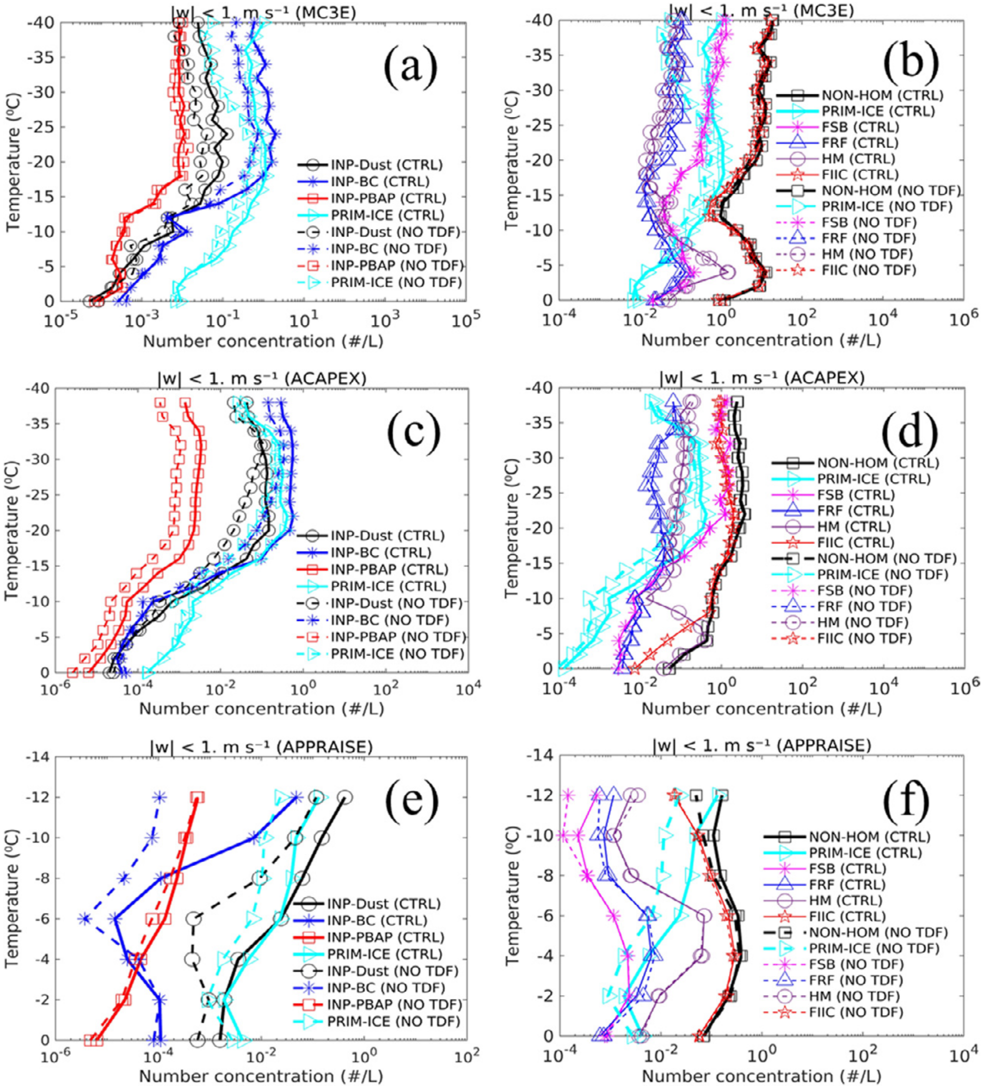

Figure 8. (left) The predicted number concentrations of active INPs conditionally averaged over stratiform regions ($|w| < 1$ m s^{-1}) from mineral dust (solid line with open circles), soot (solid line with asterisks), and PBAP (solid line with squares), and concentrations of heterogeneously nucleated ice (PRIM-ICE, forward-pointing triangles) for the (a) MC3E, (c) ACAPEX, and (e) APPRAISE cases. The same information is shown with dotted lines for the "no time-dependent INP" run. (right) The concentrations of total nonhomogeneous ice (total cloud ice and snow minus total homogeneous ice; solid line with squares) and various tracer terms defining SIP processes such as fragmentation during sublimation (FSB; solid line with asterisks), ice–ice collisions (FIIC; solid line with pentagrams) and raindrop freezing (FRF; solid line with upward-pointing triangles), and the HM process (HM; solid line with open circles) for the (b) MC3E, (d) ACAPEX, and (f) APPRAISE case, respectively. The same information is shown with the dotted lines for the "no time-dependent INP" run. To compare the number concentrations of heterogeneously nucleated ice and total nonhomogeneous ice, heterogeneously nucleated ice (PRIM-ICE; forward-pointing triangles) is also shown in the right column (adopted from Wa23a).

The conclusions of this paper are as follows:

i. In the convective updrafts of ACAPEX and MC3E, at subzero levels warmer than −36°C, SIP (through the HM and fragmentation in ice-ice collisions) contribute about 80% (in ACAPEX, Fig. 8d) and 99% (in MC3E, Fig. 8b) to the overall ice concentration. While in their convective downdraft regions, fragmentation in sublimation form about 20-40% of the total ice concentration at these levels.

ii. For the simulated supercooled layer clouds in APPRAISE, the inclusion of time dependence in the control run predicts an increase of about 30% in the overall ice concentrations (Fig. 8f).

iii. In the episode of weak embedded convection, at subzero levels (> −15°C), the SIP activity (through the HM process and fragmentation in ice-ice collisions) initiates about 75% of the overall ice concentration.

iv. By contrast, in the layer cloud episode of such clouds, the overall ice concentration is mostly dominated by heterogeneously nucleated ice (about 80% of the total ice concentration) whereas, in such clouds, the SIP activity is relatively weak, initiating only about 20% of the overall ice concentration. This is mainly due to relatively weak vertical velocities (few cm s^{-1}) and low water contents of cloud-liquid and ice-crystals in such clouds.

v. Also, in the layer cloud episode, it is further predicted that droplets falling from the upper cloudy layer (−7 to −15°C) in the subsaturation region (0 to −7°C) evaporates and releases dust particles embedded in them. These dust particles form about 45% of the total dust mass in the subsaturated region. These dust particles, following weak vertical motions, may reactivate and nucleate ice once they reach the upper mixed-phase cloudy layer (−7 to −15°C).

vi. This reactivation following the recirculation of dust particles in such long-lived layer clouds is predicted to happen over 1-2 hours, which is less than the time (> 10 hours) required for time-dependent INP freezing to alter the predicted overall ice concentration appreciably.

vii. Hence, in the long-lived layer cloud episode of APPRAISE, the recirculation and reactivation of dust particles is the main source for continuous ice nucleation and precipitation production, and not the time dependence of INP freezing, as claimed by WI13.

To conclude, for the simulated cases (APPRAISE, ACAPEX, and MC3E), this paper suggests that, the presence of time dependence cause only a slight increase, by about 10-30%, in the overall ice concentration. In ACAPEX and MC3E, and in weak embedded convection episode of the APPRAISE, SIP is the main source for the quasi-steady state of ice formation and precipitation. However, in the layer cloud episodes of APPRAISE, reactivation following the recirculation of dust INPs is the main cause of continuous ice nucleation and precipitation. This recycling of INPs is consistent with previous studies such as those by Fan et al. (2009) and Raatikainen et al. (2022). Hence, the time dependence of INP freezing can be neglected in numerical simulations of natural clouds. More details are from Wa23a.

6.3 Paper 3

Dependencies of Four Mechanisms of Secondary Ice Production on Cloud-Top temperature in a Continental Convective Storm.

In this paper, the dependency of various SIP mechanisms (Sec. 1.1.2) on cloud top temperature and their evolution with time in the simulated continental deep convection (MC3E 11 May 2011) have been studied. A measure of SIP is defined using the term known as the IE ratio which in the present study is defined as the ratio between the number concentrations of the total non-homogeneously nucleated ice and active INPs. Based on this metric, the development of convective clouds to become cumulonimbi is expected to exhibit a corresponding evolution in the overall intensity of ice multiplication (Sec. 1.1.2). Also, the activity of various SIP mechanisms is predicted to evolve with the age of the clouds. It is predicted that in the simulated deep convection (MC3E), at subzero levels warmer than −36°C, the overall ice concentration is chiefly from SIP (about 80-95% of the total ice).

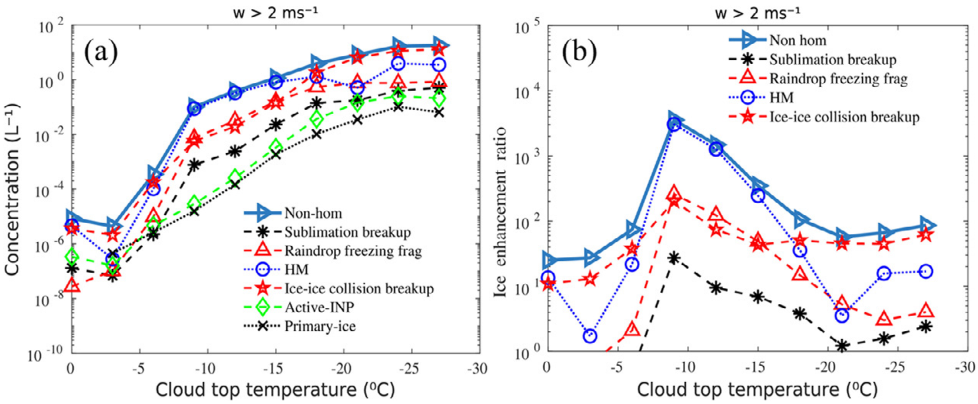

Figure 9. (a) Conditionally averaged ($w > 2$ m s^{-1}) predictions of concentrations of the active INPs (diamonds), primary ice (crosses), total nonhomogeneous ice (total ice from cloud ice and snow minus total homogeneous ice) (right-pointing triangles) as a function of cloud top temperatures and ice concentrations from various SIP processes tracked using tagging tracers such as the HM process (circles) and fragmentation during ice-ice collisions (stars), raindrop freezing (upward-pointing triangles), and sublimation of dendritic snow and graupel (asterisks). All these concentrations are at temperatures warmer than (by 1 to 7°C) the cloud top. All the terms are the geometric means of non-zero values. Also shown is a profile of (b) the predicted IE ratio as a function of cloud top temperature for convective cloudy updraft regions ($w > 2$ m s^{-1}) of the simulated MC3E (11 May 2011) clouds sampled using the cloud-top algorithm (Wa22, Appendix A).

The conclusions of this paper are as follows:

i. In the simulated deep convection (MC3E), the IE ratios are typically between 10 and 10^3 and are dependent on cloud-top temperatures (Fig. 9b). Furthermore, these IE ratios are mostly dominated by young developing convective turrets with top temperatures between −4 and −20ºC.

ii. Also, the simulated IE ratios are between 10 and 10^3 for cloud tops between 0 and −30ºC with a peak (10^3) at about −10ºC and a minimum (about 50) at cloud tops of about −20ºC. These predicted IE ratios are consistent with the previous aircraft study of a summertime continental convective storm by Hobbs et al. (1980) who reported a peak in IE ratio at cloud-top of about −12ºC.

iii. For such deep convection with relatively warm bases (17ºC), in young developing convective clouds (with tops warmer than −15ºC), the HM process of rime-splintering is predicted to dominate (about 70%) the overall ice concentration (Fig. 9a), creating IE ratios as high as 10^3. By contrast, fragmentation in ice-ice collisions prevails in typically less young convective clouds with tops colder than −20ºC, contributing more than 80% of the overall ice concentration there with IE ratios of about 10^2-10^3 (Fig. 9b).

iv. In convection (updrafts and downdrafts), SIP from fragmentation in ice-ice collisions prevails and forms more than 70% of the total ice concentrations. In downdrafts, fragmentation during sublimation is the second most dominant mechanism of ice multiplication, creating an IE ratio of about 10^2.

v. The simulated IE ratios increase with increasing convective ascent or descent and decrease with decreasing cloud top temperatures down to −22ºC.

vi. During the evolution of the simulated storm, in typically young convective turrets (tops > −15ºC), the initial explosive growth of ice concentrations is mainly from the fast HM process of rime-splintering which is consistent with Yano and Phillips (2011).

vii. According to their order of importance in initiating total ice in young developing convective clouds, the HM process can be ranked as the first, fragmentation during ice-ice collisions as the second, during raindrop freezing as the third, and during sublimation as the fourth most prolific SIP mechanism.

viii. In mature convective clouds (tops < −40ºC), fragmentation in ice-ice collisions is the first most prolific SIP process whereas the HM process is the second, raindrop freezing fragmentation is the third, and fragmentation during sublimation is the fourth important SIP process.

To summarize, this study adequately predicts the observed (Hobbs et al., 1980) classic dependency of IE ratio on cloud top temperature in young, developing convective clouds observed during MC3E (11 May 2011). In the simulated storm, the IE ratio peaks (~ 10^3) at a characteristic cloud top temperature of about -10^{o}C, which is consistent with the observations by Hobbs et al. (1980). It is further predicted that SIP (through the HM process of rime-splintering and fragmentation in ice-ice collisions) is the main cause for the explosive growth of ice concentrations, accounting for this pattern of IE ratio. This study also highlights that the age of the cloud, as it goes through its lifecycle, is of paramount importance for the relative balance of activities among various SIP mechanisms. More details are from Wa22.

6.4 Paper 4

Mechanisms for Indirect Effects from Solid Aerosol Particles on Continental Clouds and Radiation.

This paper investigates the mechanisms of the AIE from INPs in the simulated wintertime supercooled layer clouds during APPRAISE (18 February 2009) and summertime deep convective clouds during MC3E (11 May 2011). It is predicted that, in both cases, the inclusion of anthropogenic solid APs causes a decrease in the mean sizes of cloud droplets and ice crystals by about 15-30% at all cloudy levels whereas their number concentration increases by the same fraction. Also, for APPRAISE, anthropogenic INPs cause an increase of about 1% in the surface accumulated precipitation, mainly from the ice-crystal process (about 10% increase) being boosted.

Also, the contribution from the warm rain process to the surface precipitation is weakened by about 8%, mainly due to the relatively small sizes of cloud droplets. By contrast, for MC3E control runs, the inclusion of anthropogenic INPs predicts a decrease of about 1.5% in the surface precipitation due to the corresponding weakening in the precipitation from the warm rain and ice crystal processes, for the reasons noted above. This aerosol sensitivity of the precipitation also significantly alters the extents and optical thicknesses of the simulated clouds. For both cases, the inclusion of anthropogenic INPs causes an increase of about 1-3% in the horizontal and volumetric extent whereas their optical thicknesses increase by about 4% (in APPRAISE) and by 30% (in MC3E) due to weakened removal of condensate by precipitation.

In both simulations, anthropogenically increased solid aerosols significantly affect the net AIE, mainly from glaciated clouds (about 80% of the net AIE) whereas liquid-only clouds contribute only about 20% to the net AIE (Fig. 10a-d). In APPRAISE (layer-clouds) the net AIE is a cloud albedo indirect effect (cooling) since precipitation is so weak. By contrast, in MC3E (deep convection), the net AIE is chiefly from the lifetime effect (warming). Furthermore, this study also analyses the impact on the simulated AIEs from ice initiation processes such as SIP and time-dependent INP freezing.

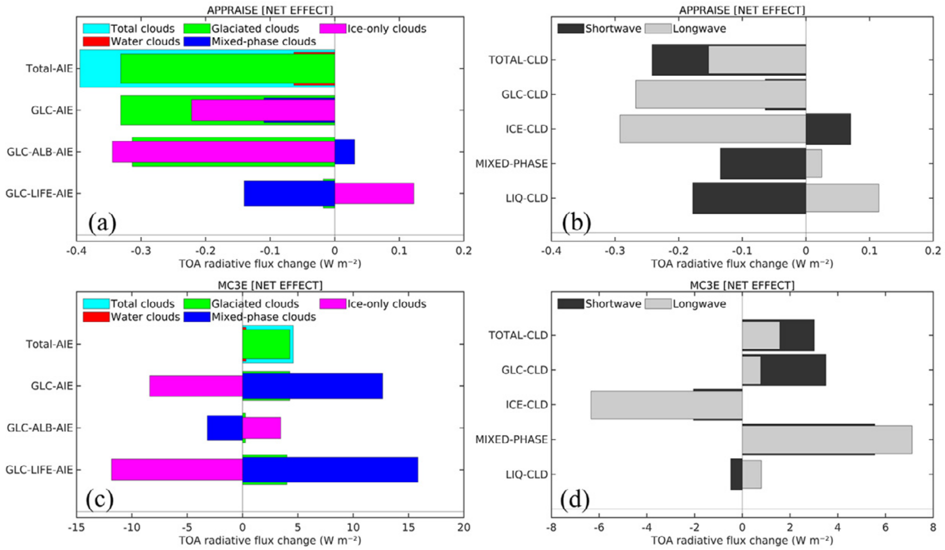

Figure 10. Net aerosol indirect effects at the TOA from solid aerosols on glaciated clouds predicted from Tests A and B (Sec. 5.4) from the control simulations of (a) APPRAISE and (c) MC3E cases. Corresponding changes in the shortwave and longwave components of radiation, unconditionally averaged over the whole domain, at the TOA, are shown for (b) APPRAISE and (d) MC3E cases. Here, abbreviations: GLC-AIE= Glaciated Clouds AIE, GLC-ALB-AIE= Glaciated cloud Albedo-Emissivity AIE, GLC-LIFE-AIE= Glaciated Cloud Lifetime AIE (Adopted from Wa23b).

The conclusions of this study are as follows:

1) For supercooled layer clouds in APPRAISE, at the TOA:

i. In the control run (Fig. 10a), anthropogenic solid APs exert a net cooling, with a net AIE of about −0.4 W m^{-2} which is dominated by the albedo-emissivity AIE from glaciated clouds (−0.3 W m^{-2}). This is mainly because increased reflectivity of such clouds due to more numerous cloud droplets and ice crystals, as discussed above.

ii. Furthermore, this net cooling is mostly due to more reflection (−0.24 W m^{-2}) of downward SW flux to space from optically thick liquid-only and mixed-phase clouds. Moreover, being optically thinner, ice-only clouds allow more LW (−0.3 W m^{-2}) radiation to leave the climate system at the TOA (Fig. 10b).

iii. By contrast, the lifetime AIE (−0.018 W m^{-2}) from such clouds is relatively low (about 5% of the net AIE), chiefly due to the weakness of precipitation from such thin layer clouds. This causes a weaker aerosol sensitivity of their horizontal and volumetric extents and of the surface precipitation than in the microphysical properties of these clouds.

iv. Also, artificially prohibiting SIP from such clouds has only a slight impact (about a 2% decrease) on the net AIE from anthropogenic solid aerosols. This is because of the relative weakness of SIP processes in such clouds (Wa23b).

v. Furthermore, in such layer clouds, when time-dependent INP freezing is prohibited, the net AIE from anthropogenic solid APs is weakened to about 65% of its control value (-0.4 W m^{-2}). This weakening is chiefly from the artificially increased reflection of the incoming SW flux from liquid-only (-0.26 W m^{-2}) and mixed-phase (-0.2 W m^{-2}) clouds as they become optically thicker in the present-day condition.

2) For summertime deep convection (MC3E, 11 May 2011), at the TOA:

i. In the control run, anthropogenic solid APs exert a net warming (4.5 W m^{-2}) of the climate system (Fig. 10c) and is mainly from the lifetime AIE from glaciated clouds (4.3 W m^{-2}). This net warming from such deep convective clouds is consistent with a previous modelling study by Fan et al. (2012).

ii. Also, this net AIE is chiefly because the inclusion of anthropogenic INPs causes mixed-phase clouds to be less extensive, allowing more downward SW flux (5.5 W m^{-2}) to enter the climate system (Fig. 10d). Also, these clouds are optically thicker, causing more partial emission of LW flux (7 W m^{-2}) to the surface, and less emission of outgoing LW radiation to space (Fig. 10d). But overall, the solar warming by mixed-phase cloud changes are more important, as longwave effects cancel out partially among cloud types in MC3E.

iii. In such deep convective clouds, by artificially prohibiting SIP, anthropogenic INPs cause a sharp decrease (by 52%) in the net warming predicted (2.2 W m^{-2}) in the control run (4.5 W m^{-2}). Also, without SIP, the overall AIE (2.2 W m^{-2}) is mainly dominated by the lifetime AIE from glaciated clouds (7 W m^{-2}). Also, both with and without SIP, anthropogenic INPs cause mixed-phase clouds to grow less extensive (by about 3%), allowing more downward SW flux (6-9 W m^{-2}) to enter the climate system.

iv. Also, when time dependence is artificially prohibited from such deep convective clouds, extra INPs cause a weak climate warming (1 W m^{-2}), which, when time dependence is included, would increase by 80% (4.58 W m^{-2}). This is chiefly from a decrease of about 105% in the net AIE from glaciated clouds, due to the inclusion of extra INPs, when time dependence is prohibited from the control run.

v. When time dependence is artificially prohibited from the simulated deep convection, ice-only clouds become less horizontally extensive, allowing more SW flux to enter the climate system (2.3 W m^{-2}). However, this warming from ice-only clouds is canceled out by more reflection of incoming SW flux (−2.2 W m^{-2}) to space from mixed-phase clouds due to a higher mass of cloud condensate in the upper half of the mixed-phase levels.

vi. By contrast, when time dependence is included in the control run, extra INPs cause a decrease by about 10% in both horizontal and volumetric extent of mixed-phase clouds, allowing more incoming SW radiation (6 W m^{-2}) to enter the climate system. Also, being optically thicker in the present-day condition, these clouds cause more absorption of outgoing LW flux (7.5 W m^{-2}).

vii. However, with time dependence, in the presence of extra INPs, SW warming from mixed-phase clouds prevail. This is mainly because the net LW warming from mixed-phase clouds is canceled out by a net LW cooling (−6 W m^{-2}) from ice-only clouds, as they are optically thinner (Wa23b).

Additionally, this paper proposes two new indirect effects that are associated with ice formation processes. These are, 1) the 'SIP' indirect effect, and 2) the 'Time-dependent INP' indirect effect. Table 4 below summarizes the net AIE and indirect effects from ice initiation processes such as time dependent INP freezing and SIP. It is predicted that for layer clouds in APPRAISE, both SIP and time-dependent INP indirect effects are weak, forming about 0.25% and 30% of the net AIE. By contrast, for deep convective clouds in MC3E, both SIP and time-dependent INP indirect effects form about 50-80% of the net AIE.

Table 4. The net AIE for the simulated APPRAISE and MC3E clouds and the indirect effects from ice initiation processes such as SIP and time dependent INP freezing.

Simulation	Indirect effect (W m^{-2})		
	Net AIE	from ice initiation process	
		SIP	Time dependent INP freezing
APPRAISE	−0.4	−0.0005	−0.13
MC3E	4.58	2.4	3.6

To conclude, this paper found that at the TOA, increasing anthropogenic pollution of solid aerosols causes a moderate cooling of the climate system via supercooled stratiform clouds. In such wintertime layer clouds, more reflection of SW flux (from liquid-only and mixed-phase clouds) contributes about 60% to the net cooling. Furthermore, in such wintertime layer clouds, more emission of outgoing LW flux to space, from less extensive and optically thinner ice-only clouds, form about 40% of the net cooling.

On the other hand, from summertime deep convective clouds in MC3E, anthropogenically emitted solid APs cause a strong warming of the present-day climate system which is mainly dominated by more SW flux (about 80% of the net warming) entering the climate system. Furthermore, for both cases, the net AIE has a higher aerosol sensitivity from glaciated clouds. This is also true for AIEs predicted in the absence of ice initiation processes such as SIP and time dependent heterogeneous ice nucleation. Also, for MC3E, the inclusion of anthropogenic INPs causes mixed-phase clouds to exert both SW and LW warming. This is because, being optically thicker in the present-day condition, they reflect more incoming SW radiation to space, causing solar warming at the TOA. Also, these clouds, at relatively lower levels (> -36^{o}C) in the atmosphere, cause more emission of LW radiation to space than to the surface, hence LW warming of the present-day climate system at the TOA (Fig. 10d).

Generally, since they are cold, high-level clouds (e.g., cirriform) contribute to greenhouse warming as they re-emit less LW flux to space than the clear-sky atmosphere, causing a net LW warming of the troposphere and surface. This is explicable in terms of Stefan-Boltzmann law which states that the amount of energy radiated by an object is proportional to the fourth power of its temperature (Liou, 2002). However, for MC3E, the inclusion of anthropogenic INPs causes high-level clouds to allow more emission of LW flux to space (-6 W m^{-2}, Fig. 10d) at the TOA. This is because for high-level clouds in MC3E, the inclusion of anthropogenic INPs causes a decrease of about 20% in the overall ice concentration. This is explicable in terms of less upwelling of cloud droplets at cirriform levels (levels colder than -36^{o}C), due to weaker ascent (about 5%) and hence less homogeneous freezing. This reduction in the number concentrations of ice particles in such high-level clouds allows more emission of LW flux to space, despite being relatively colder than pre-industrially. This is because the cloud emissivity is reduced, with less absorption of outgoing LW radiation lost to space. In short, with lower cloud emissivity, the greenhouse warming effect of the high-level clouds is weakened, causing an LW cooling of the troposphere. Also, being optically thicker in the present-day conditions (Wa23b, their Fig. 3h), such high-level clouds reflect more incoming SW radiation to space, resulting in a net solar cooling (-2 W m^{-2}).

Finally, this study concludes that anthropogenically boosted solid aerosols can significantly affect the micro- and macrophysical and hence the radiative properties of glaciated clouds. Also, SIP and time-dependent INP freezing can have a higher (up to 80% change) aerosol-sensitivity of the simulated net AIEs. More details are given by Wa23b.

7. Key Findings

- In continental conditions, the ice nucleus activity of PBAPs is weak compared to the relative activities of other INPs such as mineral dust.
- The time dependence of heterogeneous ice nucleation has a negligible contribution to the overall ice concentration in the simulated cloud systems.
- Both MC3E and ACAPEX clouds involved deeper clouds (tops as cold as −36ºC) with more intense precipitation through ice crystal process, driving more vigorous SIP.
- For APPRAISE, when weak embedded convection was present, various SIP processes are responsible for the quasi-steady ice formation and precipitation over long periods of many hours in the wintertime stratiform clouds.
- In layer cloud episode of APPRAISE, SIP is relatively weak and reactivation following recirculation of dust particles is the main source for the observed continuous ice nucleation and precipitation and not the time dependence of INP freezing.
- The concerted combination of various SIP processes adequately explains the observed discrepancy between the number concentrations of the available active INPs and the total ice particles in the simulated clouds.
- The dependency of IE ratio on cloud top temperature in different stages of the convective clouds is strongly dependent on various SIP mechanisms. In young developing convective clouds, the rapid glaciation is mainly from the relatively fast HM process whereas in mature convective clouds, fragmentation in ice-ice collisions prevails over longer times.
- In APPRAISE and MC3E, anthropogenically increased solid APs, through their INP and CCN activity, can significantly affect the micro- and macrophysical and hence radiative properties. Also, for such clouds, the presence of ice formation processes such as SIP and time dependent INP freezing has a great impact on the simulated net AIEs (about 50-80% increase).
- For the simulated APPRAISE clouds, the net AIE is about −0.39 W m^{-2}. Also, the SIP and time-dependent INP indirect effects are about −0.0005

and −0.13 W m^{-2} respectively. For deep convective clouds in MC3E, the net AIE is 4.58 W m^{-2} whereas the SIP and time-dependent INP indirect effects are about 2.4 and 3.6 W m^{-2} respectively.

- Thus, for deep convection, both SIP and time dependence of INP activity act together to amplify the indirect effect from anthropogenic solid APs, which is predominantly solar warming from mixed-phase clouds becoming less extensive as precipitation from the ice crystal process intensifies, exhibiting the lifetime effect.
- This study disproved the hypothesis that PBAP INPs can greatly affect the micro- (Sec. 2A[i]) and macrophysical (Sec. 2A[ii]) properties of the simulated MC3E clouds. Also, in the simulated clouds (APPRAISE, MC3E, and ACAPEX), the hypothesis that the time dependence of INP freezing forms the overall ice concentrations (Sec. 2B[i]) and is the main cause for the quasi-steady state of ice nucleation and precipitation (Sec. 2B[ii]) are disproved.
- For MC3E clouds, the hypothesis that various SIP processes can form the observed number concentration of ice particles in the simulated clouds is verified (Sec. 2C[i]). Also, the hypothesis that the evolution of various SIP processes strongly depends on the cloud-top temperature is verified (Sec. 2C[ii]). This study also numerically verified the aircraft observed classic dependency of IE ratio on cloud-top temperature in convective clouds (Sec. 2C[iii]).
- Moreover, the hypothesis that anthropogenically increased solid APs, via glaciated clouds, can significantly alter the micro-, macrophysical and radiative properties of the simulated clouds is verified in the present study (Sec. 2D[i, ii]). It is also verified that SIP and time dependence of INP freezing can greatly alter the radiative properties of the simulated clouds (Sec. 2D[iii]).

8. Bibliography

Albrecht, B. A., 1989. Aerosols, cloud microphysics, and fractional cloudiness, *Science*, 245, 1227– 1230.

Ansmann, A., Tesche, M., Althausen, D., Müller, D., Seifert, P., Freudenthaler, V., Heese, B., Wiegner, M., Pisani, G., Knippertz, P. and Dubovik, O., 2008. Influence of Saharan dust on cloud glaciation in southern Morocco during the Saharan Mineral Dust Experiment. *Journal of Geophysical Research: Atmospheres*, *113*(D4).

Bacon, N.J., Swanson, B.D., Baker, M.B. and Davis, E.J., 1998. Breakup of levitated frost particles. *Journal of Geophysical Research: Atmospheres*, *103*(D12), pp.13763-13775.

Blyth, A.M. and Latham, J., 1993. Development of ice and precipitation in New Mexican summertime cumulus clouds. *Quarterly Journal of the Royal Meteorological Society*, *119*(509), pp.91-120.

Bond, T.C., Doherty, S.J., Fahey, D.W., Forster, P.M., Berntsen, T., DeAngelo, B.J., Flanner, M.G., Ghan, S., Kärcher, B., Koch, D. and Kinne, S., 2013. Bounding the role of black carbon in the climate system: A scientific assessment. *Journal of geophysical research: Atmospheres*, *118*(11), pp.5380-5552.

Boucher, O., D. Randall, P. Artaxo, C. Bretherton, G. Feingold, P. Forster, V.-M. Kerminen, Y. Kondo, H. Liao, U. Lohmann, P. Rasch, S.K. Satheesh, S. Sherwood, B. Stevens and X.Y. Zhang, 2013: Clouds and Aerosols. In: Climate Change 2013: The Physical Science Basis. Contribution of Working Group I to the Fifth Assessment Report of the Intergovernmental Panel on Climate Change [Stocker, T.F., D. Qin, G.-K. Plattner, M. Tignor, S.K. Allen, J. Boschung, A. Nauels, Y. Xia, V. Bex and P.M. Midgley (eds.)]. Cambridge University Press, Cambridge, United Kingdom and New York, NY, USA.

Cantrell, W. and Heymsfield, A., 2005. Production of ice in tropospheric clouds: A review. *Bulletin of the American Meteorological Society*, *86*(6), pp.795-808.

Charlson, R.J., Schwartz, S.E., Hales, J.M., Cess, R.D., Coakley Jr, J.A., Hansen, J.E. and Hofmann, D.J., 1992. Climate forcing by anthropogenic aerosols. *Science*, *255*(5043), pp.423-430.

Chen, J.P., Hazra, A. and Levin, Z., 2008. Parameterizing ice nucleation rates using contact angle and activation energy derived from laboratory data. *Atmospheric Chemistry and Physics*, *8*(24), pp.7431-7449.

Chouippe, A., Krayer, M., Uhlmann, M., Dušek, J., Kiselev, A. and Leisner, T., 2019. Heat and water vapor transfer in the wake of a falling ice sphere and its implication for secondary ice formation in clouds. *New Journal of Physics*, *21*(4), p.043043.

Christensen, M.W., Chen, Y.C. and Stephens, G.L., 2016. Aerosol indirect effect dictated by liquid clouds. *Journal of Geophysical Research: Atmospheres*, *121*(24), pp.14-636.

Clarke, A.D., Shinozuka, Y., Kapustin, V.N., Howell, S., Huebert, B., Doherty, S., Anderson, T., Covert, D., Anderson, J., Hua, X. and Moore, K.G., 2004. Size distributions and mixtures of dust and black carbon aerosol in Asian outflow: Physiochemistry and optical properties. *Journal of Geophysical Research: Atmospheres*, *109*(D15).

Crosier, J., Bower, K.N., Choularton, T.W., Westbrook, C.D., Connolly, P.J., Cui, Z.Q., Crawford, I.P., Capes, G.L., Coe, H., Dorsey, J.R. and Williams, P.I., 2011. Observations of ice multiplication in a weakly convective cell embedded in supercooled mid-level stratus. *Atmospheric Chemistry and Physics*, *11*(1), pp.257-273.

Cziczo, D.J., Froyd, K.D., Hoose, C., Jensen, E.J., Diao, M., Zondlo, M.A., Smith, J.B., Twohy, C.H. and Murphy, D.M., 2013. Clarifying the dominant sources and mechanisms of cirrus cloud formation. *Science*, *340*(6138), pp.1320-1324.

Dagan, G., Koren, I. and Altaratz, O., 2015. Aerosol effects on the timing of warm rain processes. *Geophysical Research Letters*, *42*(11), pp.4590-4598.

DeMott, P.J., 1990. An exploratory study of ice nucleation by soot aerosols. *Journal of Applied Meteorology and Climatology*, *29*(10), pp.1072-1079.

DeMott, P.J., Finnegan, W.G. and Grant, L.O., 1983. An application of chemical kinetic theory and methodology to characterize the ice nucleating properties of aerosols used for weather modification. *Journal of Applied Meteorology and Climatology*, *22*(7), pp.1190-1203.

DeMott, P.J., Sassen, K., Poellot, M.R., Baumgardner, D., Rogers, D.C., Brooks, S.D., Prenni, A.J. and Kreidenweis, S.M., 2003. African dust aerosols as atmospheric ice nuclei. *Geophysical Research Letters*, *30*(14).

Deshmukh, A., Phillips, V.T., Bansemer, A., Patade, S. and Waman, D., 2022. New empirical formulation for the sublimational breakup of graupel and dendritic snow. *Journal of the Atmospheric Sciences*, *79*(1), pp.317-336.

Després, V., Huffman, J.A., Burrows, S.M., Hoose, C., Safatov, A., Buryak, G., Fröhlich-Nowoisky, J., Elbert, W., Andreae, M., Pöschl, U. and Jaenicke, R., 2012. Primary biological aerosol particles in the atmosphere: a review. *Tellus B: Chemical and Physical Meteorology*, *64*(1), p.15598.

Dong, Y., Oraltay, R.G. and Hallett, J., 1994. Ice particle generation during evaporation. *Atmospheric research*, *32*(1-4), pp.45-53.

Dudhia, J., 1989. Numerical study of convection observed during the winter monsoon experiment using a mesoscale two-dimensional model. *Journal of Atmospheric Sciences*, *46*(20), pp.3077-3107.

Dye, J.E. and Hobbs, P.V., 1968. The influence of environmental parameters on the freezing and fragmentation of suspended water drops. *Journal of Atmospheric Sciences*, *25*(1), pp.82-96.

Eidhammer, T., DeMott, P.J., Prenni, A.J., Petters, M.D., Twohy, C.H., Rogers, D.C., Stith, J., Heymsfield, A., Wang, Z., Pratt, K.A. and Prather, K.A., 2010. Ice initiation by aerosol particles: Measured and predicted ice nuclei concentrations versus measured ice crystal concentrations in an orographic wave cloud. *Journal of the Atmospheric Sciences*, *67*(8), pp.2417-2436.

Ervens, B., 2015. Modeling the processing of aerosol and trace gases in clouds and fogs. *Chemical reviews*, *115*(10), pp.4157-4198.

Fan, J., Ovtchinnikov, M., Comstock, J.M., McFarlane, S.A. and Khain, A., 2009. Ice formation in Arctic mixed-phase clouds: Insights from a 3-D cloud-resolving model with size-resolved aerosol and cloud microphysics. *Journal of Geophysical Research: Atmospheres*, *114*(D4).

Fan, J., Rosenfeld, D., Ding, Y., Leung, L.R. and Li, Z., 2012. Potential aerosol indirect effects on atmospheric circulation and radiative forcing through deep convection. *Geophysical Research Letters*, *39*(9).

Field, P.R. and Heymsfield, A.J., 2015. Importance of snow to global precipitation. *Geophysical Research Letters*, *42*(21), pp.9512-9520.

Field, P.R., Heymsfield, A.J. and Bansemer, A., 2006. Shattering and particle interarrival times measured by optical array probes in ice clouds. *Journal of Atmospheric and Oceanic Technology*, *23*(10), pp.1357-1371.

Field, P.R., Lawson, R.P., Brown, P.R., Lloyd, G., Westbrook, C., Moisseev, D., Miltenberger, A., Nenes, A., Blyth, A., Choularton, T. and Connolly, P., 2017. Secondary ice production: Current state of the science and recommendations for the future. *Meteorological Monographs*, *58*, pp.7-1.

Flossmann, A.I., 1998. Interaction of aerosol particles and clouds. *Journal of the atmospheric sciences*, *55*(5), pp.879-887.

Flossmann, A.I., Manton, M.J., Abshaev, A., Bruintjet, R., Murakami, M., Prabhakaran, T. and Yao, Z., 2018. *Peer review report on global precipitation enhancement activities* (Doctoral dissertation, WMO).

Fornea, A.P., Brooks, S.D., Dooley, J.B. and Saha, A., 2009. Heterogeneous freezing of ice on atmospheric aerosols containing ash, soot, and soil. *Journal of Geophysical Research: Atmospheres*, *114*(D13).

Freidenreich, S.M. and Ramaswamy, V., 1999. A new multiple-band solar radiative parameterization for general circulation models. *Journal of Geophysical Research: Atmospheres*, *104*(D24), pp.31389-31409.

Fridlind, A.M., Li, X., Wu, D., van Lier-Walqui, M., Ackerman, A.S., Tao, W.K., McFarquhar, G.M., Wu, W., Dong, X., Wang, J. and Ryzhkov, A., 2017. Derivation of aerosol profiles for MC3E convection studies and use in simulations of the 20 May squall line case. *Atmospheric Chemistry and Physics*, *17*(9), pp.5947-5972.

Gao, W., Xue, L., Liu, L., Lu, C., Yun, Y. and Zhou, W., 2021. A study of the fraction of warm rain in a pre-summer rainfall event over South China. *Atmospheric Research*, *262*, p.105792.

Gayatri, K., Patade, S., Fan, J. and Prabhakaran, T., 2022. Pathways of precipitation formation in different thermodynamic and aerosol environments over the Indian Peninsula. *Atmospheric Research*, *266*, p.105934.

Georgakaki, P., Sotiropoulou, G., Vignon, É., Billault-Roux, A.C., Berne, A. and Nenes, A., 2022. Secondary ice production processes in wintertime alpine mixed-phase clouds. *Atmospheric Chemistry and Physics*, *22*(3), pp.1965-1988.

Gettelman, A., Kay, J.E. and Shell, K.M., 2012. The evolution of climate sensitivity and climate feedbacks in the Community Atmosphere Model. *Journal of Climate*, *25*(5), pp.1453-1469.

Grabowski, W.W., Wu, X. and Moncrieff, M.W., 1999. Cloud resolving modeling of tropical cloud systems during Phase III of GATE. Part III: Effects of cloud microphysics. *Journal of the atmospheric sciences*, *56*(14), pp.2384-2402.

Griggs, D.J. and Choularton, T.W., 1983. Freezing modes of riming droplets with application to ice splinter production. *Quarterly Journal of the Royal Meteorological Society*, *109*(459), pp.243-253.

Gupta, A.K., Deshmukh, A., Waman, D., Patade, S., Jadav, A., Phillips, V.T., Bansemer, A., Martins, J.A. and Gonçalves, F.L., 2023. The microphysics of the warm-rain and ice crystal processes of precipitation in simulated continental convective storms. *Communications Earth & Environment*, *4*(1), p.226.

Hallett, J. and Mossop, S.C., 1974. Production of secondary ice particles during the riming process. *Nature*, *249*(5452), pp.26-28.

Hallett, J., Sax, R.I., Lamb, D. and Murty, A.R., 1978. Aircraft measurements of ice in Florida cumuli. *Quarterly Journal of the Royal Meteorological Society*, *104*(441), pp.631-651.

Harris-Hobbs, R.L. and Cooper, W.A., 1987. Field evidence supporting quantitative predictions of secondary ice production rates. *Journal of Atmospheric Sciences*, *44*(7), pp.1071-1082.

Hartmann, D.L., Ockert-Bell, M.E. and Michelsen, M.L., 1992. The effect of cloud type on Earth's energy balance: Global analysis. *Journal of Climate*, *5*(11), pp.1281-1304.

Hartmann, S., Seidel, J., Keinert, A., Kiselev, A., Leisner, T. and Stratmann, F., 2023. *Secondary ice production-No evidence of a productive rime-splintering mechanisms during dry and wet growth* (No. EGU23-11199). Copernicus Meetings.

Haywood, J. and Boucher, O., 2000. Estimates of the direct and indirect radiative forcing due to tropospheric aerosols: A review. *Reviews of geophysics*, *38*(4), pp.513-543.

Heymsfield, A. and Willis, P., 2014. Cloud conditions favoring secondary ice particle production in tropical maritime convection. *Journal of the Atmospheric Sciences*, *71*(12), pp.4500-4526.

Hill, A.A. and Dobbie, S., 2008. The impact of aerosols on non-precipitating marine stratocumulus. II: The semi-direct effect. *Quarterly Journal of the Royal Meteorological Society: A journal of the atmospheric sciences, applied meteorology and physical oceanography*, *134*(634), pp.1155-1165.

Hobbs, P.V. and Locatelli, J.D., 1969. Ice nuclei from a natural forest fire. *Journal of Applied Meteorology and Climatology*, *8*(5), pp.833-834.

Hobbs, P.V. and Radke, L.F., 1969. Cloud condensation nuclei from a simulated forest fire. *Science*, *163*(3864), pp.279-280.

Hobbs, P.V. and Rangno, A.L., 1985. Ice particle concentrations in clouds. *Journal of the atmospheric sciences*, *42*(23), pp.2523-2549.

Hobbs, P.V., 1969. Ice multiplication in clouds. *J. Atmos. Sci*, *26*(2), pp.315-318.

Hobbs, P.V., Politovich, M.K. and Radke, L.F., 1980. The structures of summer convective clouds in eastern Montana. I: Natural clouds. *Journal of Applied Meteorology and Climatology*, *19*(6), pp.645-663.

Hobbs, P.V., R. Farber, 1972. Fragmentation of ice particles in clouds. *J. Rech. Atmos.*, *6*, pp.245-258.

Hong, S.Y. and Pan, H.L., 1996. Nonlocal boundary layer vertical diffusion in a medium-range forecast model. *Monthly weather review*, *124*(10), pp.2322-2339.

Hoose, C. and Möhler, O., 2012. Heterogeneous ice nucleation on atmospheric aerosols: a review of results from laboratory experiments. *Atmospheric Chemistry and Physics*, *12*(20), pp.9817-9854.

Houghton, J.T., Ding, Y.D.J.G., Griggs, D.J., Noguer, M., van der Linden, P.J., Dai, X., Maskell, K. and Johnson, C.A., 2001. *Climate change 2001*.

Huang, Y., Blyth, A.M., Brown, P.R., Choularton, T.W. and Cui, Z., 2017. Factors controlling secondary ice production in cumulus clouds. *Quarterly Journal of the Royal Meteorological Society*, *143*(703), pp.1021-1031.

Jaenicke, R., 2005. Abundance of cellular material and proteins in the atmosphere. *Science*, *308*(5718), pp.73-73.

Jakobsson, J.K., Waman, D.B., Phillips, V.T. and Bjerring Kristensen, T., 2022. Time dependence of heterogeneous ice nucleation by ambient aerosols: laboratory observations and a formulation for models. *Atmospheric Chemistry and Physics*, *22*(10), pp.6717-6748.

James, R.L., Phillips, V.T. and Connolly, P.J., 2021. Secondary ice production during the break-up of freezing water drops on impact with ice particles. *Atmospheric Chemistry and Physics*, *21*(24), pp.18519-18530.

Jefferson, A., 2011. Aerosol observing system (AOS) handbook. *ARMTR-014, US Dep. of Energy, Washington, DC*, *10*.

Jensen, M.P., Petersen, W.A., Bansemer, A., Bharadwaj, N., Carey, L.D., Cecil, D.J., Collis, S.M., Del Genio, A.D., Dolan, B., Gerlach, J. and Giangrande, S.E., 2016. The midlatitude continental convective clouds experiment (MC3E). *Bulletin of the American Meteorological Society*, *97*(9), pp.1667-1686.

Johnson, B.T., Shine, K.P. and Forster, P.M., 2004. The semi-direct aerosol effect: Impact of absorbing aerosols on marine stratocumulus. *Quarterly Journal of the Royal Meteorological Society*, *130*(599), pp.1407-1422.

Johnson, D.A. and Hallett, J., 1968. Freezing and shattering of supercooled water drops. *Quarterly Journal of the Royal Meteorological Society*, *94*(402), pp.468-482.

Kanji, Z.A., Ladino, L.A., Wex, H., Boose, Y., Burkert-Kohn, M., Cziczo, D.J. and Krämer, M., 2017. Overview of ice nucleating particles. *Meteorological Monographs*, *58*, pp.1-1.

Keinert, A., Spannagel, D., Leisner, T. and Kiselev, A., 2020. Secondary ice production upon freezing of freely falling drizzle droplets. *Journal of the Atmospheric Sciences*, *77*(8), pp.2959-2967.

Khain, A.P. and Pinsky, M., 2018. *Physical processes in clouds and cloud modeling*. Cambridge University Press.

King, M.D., Platnick, S., Menzel, W.P., Ackerman, S.A. and Hubanks, P.A., 2013. Spatial and temporal distribution of clouds observed by MODIS onboard the Terra and Aqua satellites. *IEEE transactions on geoscience and remote sensing*, *51*(7), pp.3826-3852.

Koch, D. and Del Genio, A.D., 2010. Black carbon semi-direct effects on cloud cover: review and synthesis. *Atmospheric Chemistry and Physics*, *10*(16), pp.7685-7696.

Koehler, K.A., DeMott, P.J., Kreidenweis, S.M., Popovicheva, O.B., Petters, M.D., Carrico, C.M., Kireeva, E.D., Khokhlova, T.D. and Shonija, N.K., 2009. Cloud condensation nuclei and ice nucleation activity of hydrophobic and hydrophilic soot particles. *Physical Chemistry Chemical Physics*, *11*(36), pp.7906-7920.

Koop, T., Luo, B., Tsias, A. and Peter, T., 2000. Water activity as the determinant for homogeneous ice nucleation in aqueous solutions. *Nature*, *406*(6796), pp.611-614.

Korolev, A. and Leisner, T., 2020. Review of experimental studies of secondary ice production. *Atmospheric Chemistry and Physics*, *20*(20), pp.11767-11797.

Korolev, A., Heckman, I., Wolde, M., Ackerman, A.S., Fridlind, A.M., Ladino, L.A., Lawson, R.P., Milbrandt, J. and Williams, E., 2020. A new look at the environmental conditions favorable to secondary ice production. *Atmospheric Chemistry and Physics*, *20*(3), pp.1391-1429.

Korolev, A.V., Emery, E.F., Strapp, J.W., Cober, S.G., Isaac, G.A., Wasey, M. and Marcotte, D., 2011. Small ice particles in tropospheric clouds: Fact or artifact? Airborne Icing Instrumentation Evaluation Experiment. *Bulletin of the American Meteorological Society*, *92*(8), pp.967-973.

Kudzotsa, I., Phillips, V.T. and Dobbie, S., 2016. Aerosol indirect effects on glaciated clouds. Part 2: Sensitivity tests using solute aerosols. *Quarterly Journal of the Royal Meteorological Society*, *142*(698), pp.1970-1981.

Kudzotsa, I., Phillips, V.T., Dobbie, S., Formenton, M., Sun, J., Allen, G., Bansemer, A., Spracklen, D. and Pringle, K., 2016. Aerosol indirect effects on glaciated clouds. Part I: Model description. *Quarterly Journal of the Royal Meteorological Society*, *142*(698), pp.1958-1969.

Ladino, L.A., Korolev, A., Heckman, I., Wolde, M., Fridlind, A.M. and Ackerman, A.S., 2017. On the role of ice-nucleating aerosol in the formation of ice particles in tropical mesoscale convective systems. *Geophysical research letters*, *44*(3), pp.1574-1582.

Langham, E.J. and Mason, B.J.N., 1958. The heterogeneous and homogeneous nucleation of supercooled water. *Proceedings of the Royal Society of London. Series A. Mathematical and Physical Sciences*, *247*(1251), pp.493-504.

Langmuir, I., 1948. The growth of particles in smokes and clouds and the production of snow from supercooled clouds. *Proceedings of the American Philosophical Society*, *92*(3), pp.167-185.

Lasher-Trapp, S., Leon, D.C., DeMott, P.J., Villanueva-Birriel, C.M., Johnson, A.V., Moser, D.H., Tully, C.S. and Wu, W., 2016. A multisensor investigation of rime splintering in tropical maritime cumuli. *Journal of the Atmospheric Sciences*, *73*(6), pp.2547-2564.

Lasher-Trapp, S., Scott, E.L., Järvinen, E., Schnaiter, M., Waitz, F., DeMott, P.J., McCluskey, C.S. and Hill, T.C., 2021. Observations and modeling of rime splintering in Southern Ocean cumuli. *Journal of Geophysical Research: Atmospheres*, *126*(23), p.e2021JD035479.

Lau, K.M. and Wu, H.T., 2003. Warm rain processes over tropical oceans and climate implications. *Geophysical Research Letters*, *30*(24).

Lawson, R.P., Woods, S. and Morrison, H., 2015. The microphysics of ice and precipitation development in tropical cumulus clouds. *Journal of the Atmospheric Sciences*, *72*(6), pp.2429-2445.

Leisner, T., Pander, T., Handmann, P. and Kiselev, A., 2014, July. Secondary ice processes upon heterogeneous freezing of cloud droplets. In *14th Conf. on Cloud Physics and Atmospheric Radiation*.

Leung, L.R., 2016. *ARM Cloud-Aerosol-Precipitation Experiment (ACAPEX) Field Campaign Report* (No. DOE/SC-ARM-16-012). DOE Office of Science Atmospheric Radiation Measurement (ARM) Program (United States).

Levin, E.J., DeMott, P.J., Suski, K.J., Boose, Y., Hill, T.C., McCluskey, C.S., Schill, G.P., Rocci, K., Al-Mashat, H., Kristensen, L.J. and Cornwell, G., 2019. Characteristics of ice nucleating particles in and around California winter storms. *Journal of Geophysical Research: Atmospheres*, *124*(21), pp.11530-11551.

Levine, J., 1950. *Statistical explanation of spontaneous freezing of water droplets* (No. NACA-TN-2234).

Lin, Y., Fan, J., Li, P., Leung, L.Y.R., DeMott, P.J., Goldberger, L., Comstock, J., Liu, Y., Jeong, J.H. and Tomlinson, J., 2022. Modeling impacts of ice-nucleating particles from marine aerosols on mixed-phase orographic clouds during 2015 ACAPEX field campaign. *Atmospheric Chemistry and Physics*, *22*(10), pp.6749-6771.

Liou, K.N., 2002. *An introduction to atmospheric radiation* (Vol. 84). Elsevier.

Lohmann, U. and Feichter, J., 2001. Can the direct and semi-direct aerosol effect compete with the indirect effect on a global scale?. *Geophysical Research Letters*, *28*(1), pp.159-161.

Lohmann, U. and Feichter, J., 2005. Global indirect aerosol effects: a review. *Atmospheric Chemistry and Physics*, *5*(3), pp.715-737.

Lohmann, U. and Lesins, G., 2002. Stronger constraints on the anthropogenic indirect aerosol effect. *Science*, *298*(5595), pp.1012-1015.

Lohmann, U., 2006. Aerosol effects on clouds and climate. *Space Science Reviews*, *125*, pp.129-137.

Lohmann, U., Lüönd, F. and Mahrt, F., 2016. *An introduction to clouds: From the microscale to climate*. Cambridge University Press.

Lohmann, U., Rotstayn, L., Storelvmo, T., Jones, A., Menon, S., Quaas, J., Ekman, A.M., Koch, D. and Ruedy, R., 2010. Total aerosol effect: radiative forcing or radiative flux perturbation?. *Atmospheric Chemistry and Physics*, *10*(7), pp.3235-3246.

Mason, B.J., 1996. The rapid glaciation of slightly supercooled cumulus clouds. *Quarterly Journal of the Royal Meteorological Society*, *122*(530), pp.357-365.

Matthias-Maser, S. and Jaenicke, R., 1995. The size distribution of primary biological aerosol particles with radii> 0.2 µm in an urban/rural influenced region. *Atmospheric Research*, *39*(4), pp.279-286.

Matthias-Maser, S., Brinkmann, J. and Schneider, W., 1999. The size distribution of marine atmospheric aerosol with regard to primary biological aerosol particles over the South Atlantic Ocean. *Atmospheric Environment*, *33*(21), pp.3569-3575.

Matthias-Maser, S., Obolkin, V., Khodzer, T. and Jaenicke, R., 2000. Seasonal variation of primary biological aerosol particles in the remote continental region of Lake Baikal/Siberia. *Atmospheric Environment*, *34*(22), pp.3805-3811.

Miltenberger, A.K. and Field, P.R., 2021. Sensitivity of mixed-phase moderately deep convective clouds to parameterizations of ice formation–an ensemble perspective. *Atmospheric Chemistry and Physics*, *21*(5), pp.3627-3642.

Miltenberger, A.K., Lüttmer, T. and Siewert, C., 2020. Secondary ice formation in idealised deep convection—source of primary ice and impact on glaciation. *Atmosphere*, *11*(5), p.542.

Ming, Y., Ramaswamy, V., Donner, L.J. and Phillips, V.T., 2006. A new parameterization of cloud droplet activation applicable to general circulation models. *Journal of the atmospheric sciences*, *63*(4), pp.1348-1356.

Mossop, S.C., 1985. Microphysical properties of supercooled cumulus clouds in which an ice particle multiplication process operated. *Quarterly Journal of the Royal Meteorological Society*, *111*(467), pp.183-198.

Murray, B.J., O'sullivan, D., Atkinson, J.D. and Webb, M.E., 2012. Ice nucleation by particles immersed in supercooled cloud droplets. *Chemical Society Reviews*, *41*(19), pp.6519-6554.

Murray, B.J., Wilson, T.W., Dobbie, S., Cui, Z., Al-Jumur, S.M., Möhler, O., Schnaiter, M., Wagner, R., Benz, S., Niemand, M. and Saathoff, H., 2010. Heterogeneous nucleation of ice particles on glassy aerosols under cirrus conditions. *Nature Geoscience*, *3*(4), pp.233-237.

Niedermeier, D., Shaw, R.A., Hartmann, S., Wex, H., Clauss, T., Voigtländer, J. and Stratmann, F., 2011. Heterogeneous ice nucleation: exploring the transition from stochastic to singular freezing behavior. *Atmospheric Chemistry and Physics*, *11*(16), pp.8767-8775.

Oraltay, R.G. and Hallett, J., 1989. Evaporation and melting of ice crystals: A laboratory study. *Atmospheric research*, *24*(1-4), pp.169-189.

Patade, S., Phillips, V.T., Amato, P., Bingemer, H.G., Burrows, S.M., DeMott, P.J., Goncalves, F.L., Knopf, D.A., Morris, C.E., Alwmark, C. and Artaxo, P., 2021. Empirical formulation for multiple groups of primary biological ice nucleating particles from field observations over Amazonia. *Journal of the Atmospheric Sciences*, *78*(7), pp.2195-2220.

Patade, S., Shete, S., Malap, N., Kulkarni, G. and Prabha, T.V., 2016. Observational and simulated cloud microphysical features of rain formation in the mixed phase clouds observed during CAIPEEX. *Atmospheric Research*, *169*, pp.32-45.

Patade, S., Waman, D., Deshmukh, A., Gupta, A.K., Jadav, A., Phillips, V.T., Bansemer, A., Carlin, J. and Ryzhkov, A., 2022. The influence of multiple groups of biological ice nucleating particles on microphysical properties of mixed-phase clouds observed during MC3E. *Atmospheric Chemistry and Physics*, *22*(18), pp.12055-12075.

Penner, J.E., Dong, X. and Chen, Y., 2004. Observational evidence of a change in radiative forcing due to the indirect aerosol effect. *Nature*, *427*(6971), pp.231-234.

Phillips, V.T. and Patade, S., 2022. Multiple Environmental Influences on the Lightning of Cold-Based Continental Convection. Part II: Sensitivity Tests for Its Charge Structure and Land–Ocean Contrast. *Journal of the Atmospheric Sciences*, *79*(1), pp.263-300.

Phillips, V.T., Andronache, C., Christner, B., Morris, C.E., Sands, D.C., Bansemer, A., Lauer, A., McNaughton, C. and Seman, C., 2009. Potential impacts from biological aerosols on ensembles of continental clouds simulated numerically. *Biogeosciences*, *6*(6), pp.987-1014.

Phillips, V.T., Andronache, C., Morris, C.E. and Sands, D.C., 2008. Impacts from ice-nucleating bacteria on deep convection: implications for the biosphere-atmosphere interaction in climate change. *Biogeosciences Discussions*, *5*(2), pp.1035-1067.

Phillips, V.T., Andronache, C., Sherwood, S.C., Bansemer, A., Conant, W.C., Demott, P.J., Flagan, R.C., Heymsfield, A., Jonsson, H., Poellot, M. and Rissman, T.A., 2005. Anvil glaciation in a deep cumulus updraught over Florida simulated with the Explicit Microphysics Model. I: Impact of various nucleation processes. *Quarterly Journal of the Royal Meteorological Society: A journal of the atmospheric sciences, applied meteorology and physical oceanography*, *131*(609), pp.2019-2046.

Phillips, V.T., Blyth, A.M., Brown, P.R., Choularton, T.W. and Latham, J., 2001. The glaciation of a cumulus cloud over New Mexico. *Quarterly Journal of the Royal Meteorological Society*, *127*(575), pp.1513-1534.

Phillips, V.T., Demott, P.J., Andronache, C., Pratt, K.A., Prather, K.A., Subramanian, R. and Twohy, C., 2013. Improvements to an empirical parameterization of heterogeneous ice nucleation and its comparison with observations. *Journal of the Atmospheric Sciences*, *70*(2), pp.378-409.

Phillips, V.T., Donner, L.J. and Garner, S.T., 2007. Nucleation processes in deep convection simulated by a cloud-system-resolving model with double-moment bulk microphysics. *Journal of the atmospheric sciences*, *64*(3), pp.738-761.

Phillips, V.T., Formenton, M., Bansemer, A., Kudzotsa, I. and Lienert, B., 2015. A parameterization of sticking efficiency for collisions of snow and graupel with ice crystals: Theory and comparison with observations. *Journal of the Atmospheric Sciences*, *72*(12), pp.4885-4902.

Phillips, V.T., Formenton, M., Kanawade, V.P., Karlsson, L.R., Patade, S., Sun, J., Barthe, C., Pinty, J.P., Detwiler, A.G., Lyu, W. and Tessendorf, S.A., 2020. Multiple environmental influences on the lightning of cold-based continental cumulonimbus clouds. Part I: Description and validation of model. *Journal of the Atmospheric Sciences*, *77*(12), pp.3999-4024.

Phillips, V.T., Khain, A., Benmoshe, N. and Ilotoviz, E., 2014. Theory of time-dependent freezing. Part I: Description of scheme for wet growth of hail. *Journal of the Atmospheric Sciences*, *71*(12), pp.4527-4557.

Phillips, V.T., Patade, S., Gutierrez, J. and Bansemer, A., 2018. Secondary ice production by fragmentation of freezing drops: Formulation and theory. *Journal of the Atmospheric Sciences*, *75*(9), pp.3031-3070.

Phillips, V.T., Yano, J.I. and Khain, A., 2017. Ice multiplication by breakup in ice–ice collisions. Part I: Theoretical formulation. *Journal of the Atmospheric Sciences*, *74*(6), pp.1705-1719.

Phillips, V.T., Yano, J.I., Formenton, M., Ilotoviz, E., Kanawade, V., Kudzotsa, I., Sun, J., Bansemer, A., Detwiler, A.G., Khain, A. and Tessendorf, S.A., 2017. Ice multiplication by breakup in ice–ice collisions. Part II: Numerical simulations. *Journal of the Atmospheric Sciences*, *74*(9), pp.2789-2811.

Phillips, V.T.J., Choularton, T.W., Illingworth, A.J., Hogan, R.J. and Field, P.R., 2003. Simulations of the glaciation of a frontal mixed-phase cloud with the Explicit Microphysics Model. *Quarterly Journal of the Royal Meteorological Society: A journal of the atmospheric sciences, applied meteorology and physical oceanography*, *129*(590), pp.1351-1371.

Prabhakaran, P., Kinney, G., Cantrell, W., Shaw, R.A. and Bodenschatz, E., 2019. Ice nucleation in the wake of warm hydrometeors. *arXiv preprint arXiv:1906.06129*.

Prabhakaran, P., Shawon, A.S.M., Kinney, G., Thomas, S., Cantrell, W. and Shaw, R.A., 2020. The role of turbulent fluctuations in aerosol activation and cloud formation. *Proceedings of the National Academy of Sciences*, *117*(29), pp.16831-16838.

Pruppacher, H.R. and Schlamp, R.J., 1975. A wind tunnel investigation on ice multiplication by freezing of waterdrops falling at terminal velocity in air. *Journal of Geophysical Research*, *80*(3), pp.380-386.

Pruppacher, H.R., Klett, J.D., 1997. Microphysics of clouds and precipitation.

Raatikainen, T., Prank, M., Ahola, J., Kokkola, H., Tonttila, J., and Romakkaniemi, S., 2022: The effect of marine ice-nucleating particles on mixed-phase clouds, Atmos. Chem. Phys., 22, 3763–3778, https://doi.org/10.5194/acp-22-3763-2022.

Ramanathan, V.C.P.J., Crutzen, P.J., Kiehl, J.T. and Rosenfeld, D., 2001. Aerosols, climate, and the hydrological cycle. *science*, *294*(5549), pp.2119-2124.

Rangno, A.L. and Hobbs, P.V., 2001. Ice particles in stratiform clouds in the Arctic and possible mechanisms for the production of high ice concentrations. *Journal of Geophysical Research: Atmospheres*, *106*(D14), pp.15065-15075.

Rangno, A.L., 2008. Fragmentation of freezing drops in shallow maritime frontal clouds. *Journal of the atmospheric sciences*, *65*(4), pp.1455-1466.

Rauber, R.M., Olthoff, L.S., Ramamurthy, M.K. and Kunkel, K.E., 2000. The relative importance of warm rain and melting processes in freezing precipitation events. *Journal of Applied Meteorology*, *39*(7), pp.1185-1195.

Rogers, R.R., and Yau, M.K., 1996. *A short course in cloud physics*. Elsevier.

Romakkaniemi, S., Arola, A., Kokkola, H., Birmili, W., Tuch, T., Kerminen, V.M., Räisänen, P., Smith, J.N., Korhonen, H. and Laaksonen, A., 2012. Effect of aerosol size distribution changes on AOD, CCN and cloud droplet concentration: Case studies from Erfurt and Melpitz, Germany. *Journal of Geophysical Research: Atmospheres*, *117*(D7).

Ryu, Y.H. and Min, S.K., 2022. Improving Wet and Dry Deposition of Aerosols in WRF-Chem: Updates to Below-Cloud Scavenging and Coarse-Particle Dry Deposition. *Journal of Advances in Modeling Earth Systems*, *14*(4), p.e2021MS002792.

Schill, G.P., Froyd, K.D., Bian, H., Kupc, A., Williamson, C., Brock, C.A., Ray, E., Hornbrook, R.S., Hills, A.J., Apel, E.C. and Chin, M., 2020. Widespread biomass burning smoke throughout the remote troposphere. *Nature Geoscience*, *13*(6), pp.422-427.

Shaw, R.A., Durant, A.J. and Mi, Y., 2005. Heterogeneous surface crystallization observed in undercooled water. *The Journal of Physical Chemistry B*, *109*(20), pp.9865-9868.

Skamarock, W.C., Klemp, J.B., Dudhia, J., Gill, D.O., Barker, D.M., Duda, M.G., Huang, X.Y., Wang, W. and Powers, J.G., 2008. A description of the advanced research WRF version 3. *NCAR technical note*, *475*, p.113.

Sotiropoulou, G., Sullivan, S., Savre, J., Lloyd, G., Lachlan-Cope, T., Ekman, A.M. and Nenes, A., 2020. The impact of secondary ice production on Arctic stratocumulus. *Atmospheric Chemistry and Physics*, *20*(3), pp.1301-1316.

Sotiropoulou, G., Vignon, É., Young, G., Morrison, H., O'Shea, S.J., Lachlan-Cope, T., Berne, A. and Nenes, A., 2021. Secondary ice production in summer clouds over the Antarctic coast: an underappreciated process in atmospheric models. *Atmospheric Chemistry and Physics*, *21*(2), pp.755-771.

Takahashi, C. and Yamashita, A., 1969. Deformation and fragmentation of freezing water drops in free fall. *Journal of the Meteorological Society of Japan. Ser. II*, *47*(6), pp.431-436.

Takahashi, C. and Yamashita, A., 1970. Shattering of frozen water drops in a supercooled cloud. *Journal of the Meteorological Society of Japan. Ser. II*, *48*(4), pp.373-376.

Takahashi, T. and Kawano, T., 1998. Numerical sensitivity study of rainband precipitation and evolution. *Journal of the atmospheric sciences*, *55*(1), pp.57-87.

Takahashi, T., Nagao, Y. and Kushiyama, Y., 1995. Possible high ice particle production during graupel–graupel collisions. *Journal of the atmospheric sciences*, *52*(24), pp.4523-4527.

Takemura, T., 2012. Distributions and climate effects of atmospheric aerosols from the preindustrial era to 2100 along Representative Concentration Pathways (RCPs) simulated using the global aerosol model SPRINTARS. *Atmospheric Chemistry and Physics*, *12*(23), pp.11555-11572.

Troen and Mahrt, 1986: A Simple Model of the Atmospheric Boundary Layer; Sensitivity to Surface Evaporation. Bound. Lay. Met., Vol. 37, pg. 129-148.

Twohy, C.H., DeMott, P.J., Pratt, K.A., Subramanian, R., Kok, G.L., Murphy, S.M., Lersch, T., Heymsfield, A.J., Wang, Z., Prather, K.A. and Seinfeld, J.H., 2010. Relationships of biomass-burning aerosols to ice in orographic wave clouds. *Journal of the atmospheric sciences*, *67*(8), pp.2437-2450.

Twomey, S.J.A.E., 1974. Pollution and the planetary albedo. *Atmospheric Environment (1967)*, *8*(12), pp.1251-1256.

Uin, J., 2022. *Cloud condensation nuclei particle counter (CCN) instrument handbook* (No. DOE/SC-ARM-TR-168). DOE Office of Science Atmospheric Radiation Measurement (ARM) Program (United States).

Vali, G. and Stansbury, E.J., 1966. Time-dependent characteristics of the heterogeneous nucleation of ice. *Canadian Journal of Physics*, *44*(3), pp.477-502.

Vali, G., 1985. Nucleation terminology. *Bulletin of the American Meteorological Society*, *66*(11), pp.1426-1427.

Vali, G., 1994. Freezing rate due to heterogeneous nucleation. *Journal of Atmospheric Sciences*, *51*(13), pp.1843-1856.

Vali, G., 2008. Repeatability and randomness in heterogeneous freezing nucleation. *Atmospheric Chemistry and Physics*, *8*(16), pp.5017-5031.

Vali, G., 2014. Interpretation of freezing nucleation experiments: singular and stochastic; sites and surfaces. *Atmospheric Chemistry and Physics*, *14*(11), pp.5271-5294.

Vali, G., DeMott, P.J., Möhler, O. and Whale, T.F., 2015. A proposal for ice nucleation terminology. *Atmospheric Chemistry and Physics*, *15*(18), pp.10263-10270.

Vardiman, L., 1978. The generation of secondary ice particles in clouds by crystal–crystal collision. *Journal of Atmospheric Sciences*, *35*(11), pp.2168-2180.

Vonnegut, B. and Baldwin, M., 1984. Repeated nucleation of a supercooled water sample that contains silver iodide particles. *Journal of Applied Meteorology and Climatology*, *23*(3), pp.486-490.

Waman, D., Deshmukh, A., Jadav, A., Patade, S., Gautam, M., Phillips, V., Bansemer, A. and Jakobsson, J., 2023. Effects from time dependence of ice nucleus activity for contrasting cloud types. *Journal of the Atmospheric Sciences*.

Waman, D., Deshmukh, A., Jadav, A., Patade, S., Gautam, M., Phillips, V., 2023. Mechanisms for indirect effects from solid aerosol particles on continental clouds and radiation. (Submitted to Journal of the Atmospheric Sciences).

Waman, D., Patade, S., Jadav, A., Deshmukh, A., Gupta, A.K., Phillips, V.T., Bansemer, A. and DeMott, P.J., 2022. Dependencies of Four Mechanisms of Secondary Ice Production on Cloud-Top Temperature in a Continental Convective Storm. *Journal of the Atmospheric Sciences*, *79*(12), pp.3375-3404.

Wang, Z., Schaaf, C.B., Strahler, A.H., Chopping, M.J., Román, M.O., Shuai, Y., Woodcock, C.E., Hollinger, D.Y. and Fitzjarrald, D.R., 2014. Evaluation of MODIS albedo product (MCD43A) over grassland, agriculture and forest surface types during dormant and snow-covered periods. *Remote Sensing of Environment*, *140*, pp.60-77.

Warneck, P., 1999. *Chemistry of the natural atmosphere* (Vol. 71). Elsevier.

Welti, A., Lüönd, F., Kanji, Z.A., Stetzer, O. and Lohmann, U., 2012. Time dependence of immersion freezing: an experimental study on size selected kaolinite particles. *Atmospheric Chemistry and Physics*, *12*(20), pp.9893-9907.

Westbrook, C.D. and Illingworth, A.J., 2013. The formation of ice in a long-lived supercooled layer cloud. *Quarterly Journal of the Royal Meteorological Society*, *139*(677), pp.2209-2221.

Wildeman, S., Sterl, S., Sun, C. and Lohse, D., 2017. Fast dynamics of water droplets freezing from the outside in. *Physical review letters*, *118*(8), p.084101.

Wright, T.P., Petters, M.D., Hader, J.D., Morton, T. and Holder, A.L., 2013. Minimal cooling rate dependence of ice nuclei activity in the immersion mode. *Journal of Geophysical Research: Atmospheres*, *118*(18), pp.10-535.

Yang, J., Lei, H., Hu, Z. and Hou, T., 2014. Particle size spectra and possible mechanisms of high ice concentration in nimbostratus over Hebei Province, China. *Atmospheric research*, *142*, pp.79-90.

Yang, J., Wang, Z., Heymsfield, A.J., DeMott, P.J., Twohy, C.H., Suski, K.J. and Toohey, D.W., 2020. High ice concentration observed in tropical maritime stratiform mixed-phase clouds with top temperatures warmer than− 8 C. *Atmospheric Research*, *233*, p.104719.

Yano, J.I. and Phillips, V.T.J., 2011. Ice–ice collisions: An ice multiplication process in atmospheric clouds. *Journal of the Atmospheric Sciences*, *68*(2), pp.322-333.

Yano, J.I., Phillips, V.T. and Kanawade, V., 2016. Explosive ice multiplication by mechanical break-up in ice–ice collisions: a dynamical system-based study. *Quarterly Journal of the Royal Meteorological Society*, *142*(695), pp.867-879.

Yli-Juuti, T., Mielonen, T., Heikkinen, L., Arola, A., Ehn, M., Isokääntä, S., Keskinen, H.M., Kulmala, M., Laakso, A., Lipponen, A. and Luoma, K., 2021. Significance of the organic aerosol driven climate feedback in the boreal area. *Nature communications*, *12*(1), p.5637.

Young, G., Lachlan-Cope, T., O'Shea, S.J., Dearden, C., Listowski, C., Bower, K.N., Choularton, T.W. and Gallagher, M.W., 2019. Radiative effects of secondary ice enhancement in coastal Antarctic clouds. *Geophysical Research Letters*, *46*(4), pp.2312-2321.

Zhao, X. and Liu, X., 2021. Global importance of secondary ice production. *Geophysical Research Letters*, *48*(11), p.e2021GL092581.

Zhao, X., Liu, X., Phillips, V.T. and Patade, S., 2021. Impacts of secondary ice production on Arctic mixed-phase clouds based on ARM observations and CAM6 single-column model simulations. *Atmospheric Chemistry and Physics*, *21*(7), pp.5685-5703.